ROLE OF RPB9 IN RNA POLYMERASE II FIDELITY

A Dissertation

by

KEVIN CHRISTOPHER KNIPPA

Submitted to the Office of Graduate Studies of
Texas A&M University
in partial fulfillment of the requirements for the degree of

DOCTOR OF PHILOSOPHY

Chair of Committee,	David Oscar Peterson
Committee Members,	Mary Bryk
	Paul Lindahl
	Van Wilson
Head of Department,	Gregory Reinhart

August 2013

Major Subject: Biochemistry

ABSTRACT

RNA polymerase II, the polymerase responsible for transcribing protein coding genes in eukaryotes, possesses an ability to discriminate between correct (complementary to the DNA template) and incorrect substrates (selectivity), and as well as remove incorrect substrates that have been erroneously incorporated into the nascent RNA transcript (proofreading). Although these features of pol II are not as robust as those observed for DNA polymerases, the accurate utilization of genetic information is of obvious importance to the cell. The role of the small RNA polymerase II subunit Rpb9 in transcriptional proofreading was assessed *in vitro*. Transcription elongation complexes in which the 3'-end of the RNA is not complementary to the DNA template have a dramatically reduced rate of elongation, which provides a fidelity checkpoint at which the error can be removed. The efficiency of such proofreading depends on competing rates of error propagation (extending the RNA chain without removing the error) and error excision, a process that is facilitated by TFIIS. In the absence of Rpb9, the rate of error propagation is increased by 2- to 3-fold in numerous sequence contexts, compromising the efficiency of proofreading. In addition, the rate and extent of TFIIS-mediated error excision is also significantly compromised in the absence of Rpb9. In at least some sequence contexts, Rpb9 appears to enhance TFIIS-mediated error excision by facilitating efficient formation of a conformation necessary for RNA cleavage. If a transcription error is propagated by addition of a nucleotide to the mismatched 3'-end, the rate of further elongation increases but remains much slower than that of a complex with a fully base-paired RNA, which provides a second potential fidelity checkpoint. The absence of Rpb9 also affects both error propagation and TFIIS-mediated error excision at this potential fidelity checkpoint in a manner that compromises transcriptional fidelity.

The trigger loop, a mobile structural element of the largest subunit of RNA polymerase II is important for maintaining fidelity. The pol II specific toxin α-amanitin targets the trigger loop, and was used to distinguish trigger loop -independent and -

dependent Rpb9 functions, *in vitro*. Rpb9 decreases the correct nt extension rate when trigger loop movement is restricted by α-amanitin. This occurs in the context of a RNA with a matched or mismatched 3'-end, which indicates that Rpb9's contribution to correct nt extension occurs in a manner independent of the trigger loop. In addition, the effect on mismatch extension indicates that the trigger loop is not required for Rpb9 to facilitate recognition of proofreading 'checkpoints' after mismatches occur. Rpb9 also decreases the rate of misincorporation, but this effect is dependent on the trigger loop. Rpb9's role in selectivity was tested by utilizing several assays to estimate nt discrimination. Rpb9 does not have a significant effect on nt discrimination for the sequence contexts tested, which suggests the role Rpb9 plays in fidelity is in large part due to its proofreading capabilities. Lastly, the charged residues of Rpb9's C-terminal "loop" region, proposed in the prevailing model to be important for trigger loop interaction, are dispensable for Rpb9 function *in vivo* and *in vitro*.

DEDICATION

To my mother and father

ACKNOWLEDGEMENTS

I would like to first express gratitude to Dr. David Peterson for the many years of training, guidance, advice, and unwavering support. I will always be grateful for the knowledge and insight he so generously provided me. Dave was an inspiring example of a truly good person in both scientific and personal settings. I will continue to model myself after him. I would also like to relate my sincere appreciation to my committee, Dr. Mary Bryk, Dr. Paul Lindahl, and Dr. Van Wilson for sacrificing their precious time to help advance my understanding of scientific research, and for their encouragement, helpful advice and suggestions. Lastly, I thank my family and friends for supporting me throughout this program.

TABLE OF CONTENTS

Page

ABSTRACT ii

DEDICATION iv

ACKNOWLEDGEMENTS v

TABLE OF CONTENTS vi

LIST OF FIGURES viii

NOMENCLATURE x

CHAPTER 1

I INTRODUCTION 1

Pol II transcription 2
Pol II EC architecture 3
Nucleotide addition cycle 3
Pol II fidelity 8
TFIIS and backtracking 16
Trigger loop and bridge helix 17
Rpb9 22
Rpb9 and transcriptional fidelity 26

II MATERIALS AND METHODS 28

Yeast strains, growth, and preparation of whole cell extract 28
Pol II and TFIIS purification 28
RNA labeling and RNA-DNA hybrid formation 28
Elongation complex assembly and *in vitro* transcription 29
Western blotting 30

III FIDELITY OF RNA POLYMERASE II TRANSCRIPTION: ROLE OF RBP9 IN NUCLEOTIDE DISCRIMINATION 31

Introduction 31
Results 32
Pol II derived from an *rpb9*Δ strain increases the rate of UTP for CTP errors 32
Purification of pol II 34
Absence of Rpb9 increases the rate of misincorporation 35
Absence of Rpb9 increases the rate of elongation with the correct nucleotide 38
Rpb9 and selectivity 39

Discussion 44

IV FIDELITY OF RNA POLYMERASE II TRANSCRIPTION: ROLE OF RBP9 IN ERROR DETECTION AND PROOFREADING 46

Introduction 46
Results 47
Absence of Rpb9 increases the rate of elongation beyond a mismatched 3'-end 47
Rpb9 promotes TFIIS-mediated cleavage of transcripts with a mismatched 3'-end 49
Absence of Rpb9 increases the rate of elongation beyond a mismatched-matched 3'-end 56
Rpb9 promotes TFIIS-mediated cleavage of a mismatched-matched 3'-end 57
Discussion 61

V TRIGGER LOOP –DEPENDENT AND –INDEPENDENT FUNCTIONS OF THE RNA POLYMERASE II SUBUNIT RPB9 64

Introduction 64
Results 66
Rbp9 effects on correct nucleotide extension of a matched 3'-end in the presence of α-amanitin 66
Rbp9 effects on misincorporation in the presence of α-amanitin 68
Rbp9 effects on mismatch extension in the presence of α-amanitin 68
Charged residues of Rpb9 (91-94) are dispensable both *in vivo* and *in vitro* 72
Discussion 75

VI SUMMARY 78

Future directions 81

REFERENCES 84

LIST OF FIGURES

Fig. 1.1. Structure of pol II elongation complex. 4
Fig. 1.2. Nucleotide addition cycle. 6
Fig. 1.3. Two metal mechanism of catalysis for all polymerases. 7
Fig. 1.4. Backtracking-RNA with a matched 3'-end 9
Fig. 1.5. Backtracking-RNA with a mismatched 3'-end 13
Fig. 1.6. Model for transcriptional fidelity 15
Fig. 1.7. Interconnecting models for NAC, backtracking, and proofreading 18
Fig. 1.8. NAC in the context of TL movement and α-amanitin inhibition 21
Fig. 1.9. Sequence and structure of Rpb9 25
Fig. 3.1. Misincorporation of UTP for CTP 33
Fig. 3.2. SDS polyacrylamide gel electrophoresis of purified pol II 36
Fig. 3.3. Pol IIΔ9 increases the rate of NTP misicorporation 37
Fig. 3.4. Pol IIΔ9 increases the rate of elongation 40
Fig. 3.5. NTP Selectivity 41
Fig. 3.6. Assay to determine selectivity by direct competition of CTP and UTP 43
Fig. 4.1. Effect of Rpb9 on extension of a mismatched 3'-end 48
Fig. 4.2. Effect of Rpb9 on TFIIS-mediated cleavage of a 3'-mismatched end 50
Fig. 4.3. Cleavage of mismatched 3'-ends by ECs assembled from WCE 53
Fig. 4.4. Cleavage of in situ-generated 3'-end mismatches 55
Fig. 4.5. Effect of Rpb9 on extension of a mismatch-matched 3'-end 58
Fig. 4.6. Effect of Rpb9 on proofreading a mismatch-matched 3'-end 59
Fig. 5.1. Pol IIΔ9 increases the rate of elongation in the presence of α-amanitin 67
Fig. 5.2. Pol IIΔ9 increases the rate of ATP misincorporation only in the absence of α-amanitin 69
Fig. 5.3. Pol IIΔ9 increases the rate of mismatch extension in the presence of α-amanitin 71

Fig. 5.4. Model for Rpb9 effect on selectivity 73
Fig. 5.5. Analysis of Rpb9 C-terminal loop residues 74
Fig. 6.1. Proposed model for TL-independent and TL-dependent functions of Rpb9 82

NOMENCLATURE

BH	bridge helix
bp	base pair
(d)	deoxy
DNA pol	DNA polymerase
ECs	elongation complexes
GST	glutathione-S-transferase
MPA	mycophenolic acid
NAC	nucleotide addition cycle
NER	nucleotide excision repair
nt	nucleotide
NTP	nucleoside triphosphate
pol I	RNA polymerase I
pol II	RNA polymerase II
pol III	RNA polymerase III
*rpb9*Δ	strain with a deletion of the gene encoding Rpb9
SDS-PAGE	sodium dodecyl-sulfate polyacrylamide gel electrophoresis
TB	transcription buffer
TCR	transcription coupled repair
TL	trigger loop
WCE	whole cell extract
Zn1	Rpb9 N-terminal zinc ribbon
Zn2	Rpb9 C-terminal zinc ribbon

CHAPTER I

INTRODUCTION

Transcription is the process by which RNA polymerase synthesizes RNA according to the ordered chemical structure of DNA. In eukaryotes there are three core RNA polymerases: RNA polymerase I (pol I), RNA polymerase II (pol II), and RNA polymerase III (pol III). Pol I synthesizes ribosomal RNA, whereas pol II and pol III transcribe precursor mRNA/small RNAs, and tRNAs/5S rRNA, respectively [1]. Transcription of the protein-coding genes represents the first opportunity to control gene expression. Pol II is the centerpiece of this process, which consists of three fundamental steps: initiation, elongation, and termination. At each of these steps pol II does not act alone, but coordinates with a myriad of different protein factors that can either promote or inhibit transcription [2].

Several studies argue that the rate and efficiency of transcription are important targets for regulation [3]. One critical aspect of RNA synthesis is fidelity, which relates to the efficiency of pol II to transcribe an RNA that is precisely complementary to the sequence of the template DNA. The effects of unfaithful transcription can result in truncated or mis-folded proteins that can be inactive or cause other proteins to become inactive. Importantly, because pol II transcribes all of the protein coding genes, these effects can potentially be realized in many cellular locations and processes [4, 5].

In this work, I focus on the role of the yeast (*Saccharomyces cerevisiae*) pol II subunit Rpb9 in mechanisms of transcription fidelity. *S. cerevisae* is used for these studies because it is a tractable model organism that can be grown in large quantities, allows for rapid genetic manipulation, and significantly, its pol II has functional [6] and sequence homology with all eukaryotic pol II [7].

Pol II transcription

In cellular transcription, pol II requires a DNA promoter and several general protein factors to specifically initiate transcription, which are designated TFIIA, TFIIB, TFIID, TFIIE, TFIIF, and TFIIH. These factors typically assemble at TATA-elements upstream of the transcription start site to recruit and position pol II, and facilitate DNA strand separation for initial RNA synthesis [2, 8]. After this initial synthesis, that clears pol II of the promoter region, begins the elongation phase, which is characterized by productive RNA synthesis. Pol II can, however, encounter different obstacles during the elongation phase such as DNA sequence-specific pause sites, DNA damage, or template-bound proteins, most notably in the form of the histone octamers which package DNA into chromatin. In each case, pol II can pause or arrest and may require additional protein factors to resume RNA synthesis. Another intricate feature of pol II transcription is the highly conserved C-terminal repeat domain of the Rpb1subunit, which consists of several heptapeptide repeats. These repeats are phosphorylated differentially and associate with proteins important for initiation, chromatin remodeling, and RNA processing [9].

In spite of the complexity that occurs during *in vivo* transcription, much has been learned about the composition and basic mechanisms of pol II through crystal structures of artificial elongation complexes (ECs). There are a wide variety of structures for pol II that have been captured utilizing different substrates or their analogs, or ECs assembled with transcriptional inhibitors, matched or mismatched 3'-ends, DNA lesions, or transcription factors [10]. These studies have revealed not only that pol II shares a structurally conserved active center with pol I and pol III, but also multi-subunit polymerases from other domains of life (bacteria and archaea), which suggests that a common mechanism of nucleotide (nt) addition applies to all multi-subunit polymerases [10, 11].

Pol II EC architecture

Pol II is a 500 kDa protein-complex that consists of 12-subunits termed, Rpb1-12 (Fig. 1.1). The active center of the enzyme is derived almost entirely from the two largest subunits Rpb1 and Rpb2. Together these subunits form an overall structure that resembles a "crab claw". What has been termed as the Rpb1/Rpb2 cleft cradles the DNA duplex entering the active center through the primary channel. The DNA duplex is unwound before it enters the active center and then rewound upon exiting the active center. This region of DNA strand separation, approximately 12-15 base pairs (bp), encompasses the transcription "bubble". Single strand template DNA is then free to base pair with complementary nucleotide triphosphates (NTP) [12]. Approximately 8-9 bp of RNA form a hybrid with the single strand template DNA, which along with upstream DNA takes a right angle turn at the active site relative to the incoming downstream template DNA. The 3'-end of the growing RNA stays in contact with the active center while the 5'-end of the RNA is separated from template DNA and guided through an exit channel [11, 12].

There is much debate about the path a NTP takes to gain access to the active site. The model that garners the most support is derived from structural and biochemical data. This model states that the NTP enters through the secondary channel, which consists of a funnel and pore structure beneath the active site (this channel along with the primary channel are the only two feasible entry points for NTP). Conversely, it was suggested from pre-steady state kinetic studies that NTPs bind template DNA just ahead of pol II and enter the active site through the primary channel, already base paired with single-strand template DNA [10, 11].

Nucleotide addition cycle

The addition of NTPs to the 3'-end of a growing RNA is a cyclical process that involves selection and binding of a NTP complementary to template DNA, a conformational change conducive to catalysis, phosphoryl transfer, another

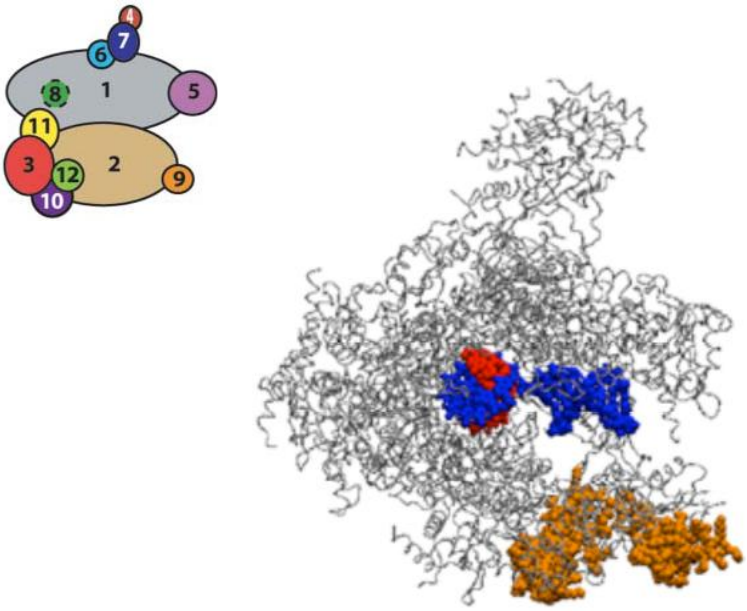

Fig. 1.1. Structure of pol II elongation complex. The structure of the 12 subunit *S. cerevisiae* elongation complex is shown in what is referred to as the top view. Space filling models represent segments of template DNA (blue) and nascent RNA (red). downstream template would stretch out to the right and upstream template would extend up and out of the page. Movement of pol II would be to the right, where the space filling model of Rpb9 (orange) highlights its position at the leading edge of the enzyme. From Protein Data Bank ID code 1Y1W.

conformational change, pyrophosphate release, and translocation. The exact order and timing of the latter steps is not clear (Fig. 1.2) [10-12].

A two-metal ion mechanism aptly describes the catalytic nt addition reaction for pol II and all multi-subunit polymerases (Fig. 1.3) [13]. RNA synthesis occurs via phosphodiester bond formation (S_N2 mechanism) facilitated by two metal ions, metal A and metal B. Metal A is stably bound to pol II and is coordinated by three highly conserved aspartate amino acids of the Rpb1 subunit. It assists in the deprotonation of the RNA 3'OH group for nucleophilic attack on the α-phosphate of the NTP. Metal B is transiently associated and is thought to enter the active site with the incoming NTP and exit with the product, pyrophosphate. The position of metal B is very close to a couple of the aspartate residues of Rpb1 that coordinate metal A, and also a highly conserved aspartate and glutamate of Rpb2 [11, 12].

Several NTP binding sites have been identified from high resolution crystal structures. Westover, K.D. *et al*. [14] used pol II ECs prepared with terminal 3'-deoxy RNA, to inhibit extension. In this structure, the correct NTP occupied a distinct position referred to as the insertion site. This site reflects a catalytically competent conformation where the NTP is base-paired with template DNA and stabilized by two metal ions. In the same study, a NTP non-complementary to the template was localized to the E site, proposed to be specific for incorrect NTP. Unlike the correct NTP in the insertion site, the nt moiety is pointed away from the template DNA in the E site. However, the phosphates are still in complex with the two metal ions [14]. Kettenberger, H. *et al*. [15] used a different approach where the complementary NTP consisted of a non-hydrolyzable triphosphate group. This scenario identified the preinsertion site, which overlaps with the insertion site. The NTP is base paired with the template DNA, yet not coordinated with the metal ions for catalysis [16]. The role of these alternative sites may involve sampling mechanisms for NTP complementary to template DNA either in transit to or from the insertion site, but could also arise from the unnatural chemical modifications used to construct the complexes [10].

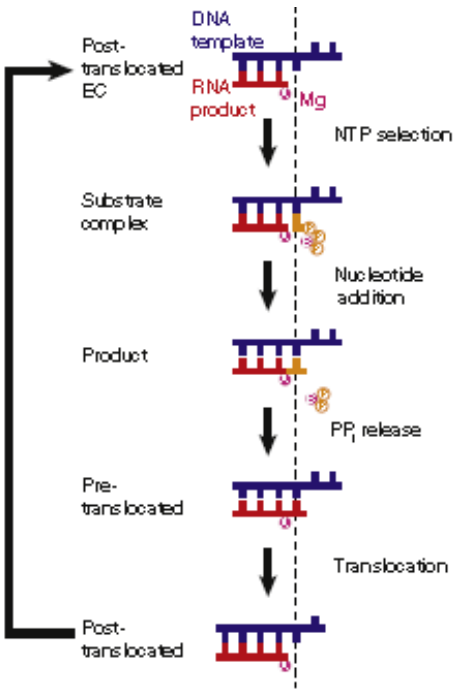

Fig. 1.2. Nucleotide addition cycle. The dashed line represents the location of the insertion site relative to the DNA/RNA hybrid. The pink circle indicates the position of the active site and the yellow circles show the phosphates of the incoming NTP. (modified from Cramer, P Biochimica et Biophysica Acta 1829 (2013) 9–19.)

\

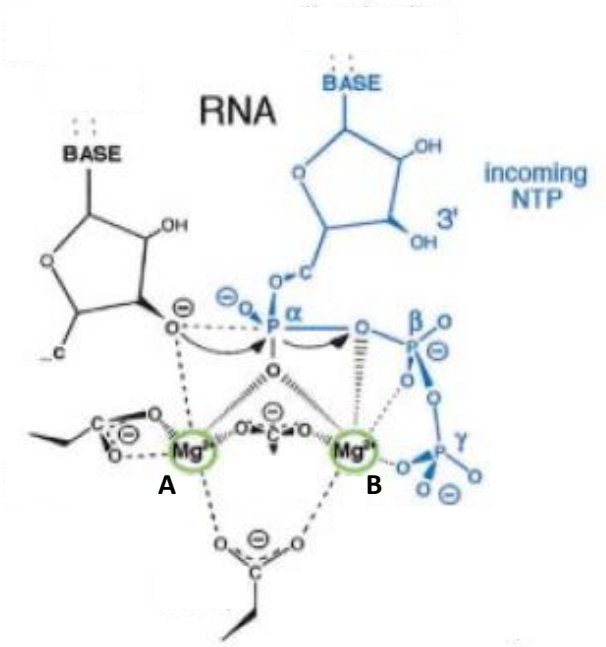

Fig. 1.3. Two metal mechanism of catalysis for all polymerases. The figure illustrates nucleophilic attack of the 3'-OH on the α-phosphate of the incoming NTP. Coordination of metal A and metal B with aspartate residues and NTP phosphates is also shown. (modified from Sosunov, V et al. EMBO J. 2003 May 1**;** 22(9): 2234–2244.)

Pol II can move forwards and backwards relative to DNA, and this motion is likely fueled by thermal fluctuations, consistent with a Brownian ratchet model, as opposed to energy derived from NTP hydrolysis. Pol II oscillates between pre-translocated, post-translocated, and backtracked states, all of which have been observed in crystal structures [10, 12]. The pre-translocated state defines a catalytically incompetent pol II where the newly formed 3'-end of the RNA occupies the insertion site. The post-translocated state is characterized by forward movement of one nt, which clears the insertion site for the next complementary NTP to bind and represents a catalytically competent conformation (see Fig. 1.2). Finally, in the backtracked state the 3'-end of the RNA is misaligned with and extrudes from the active site. The time that pol II resides in the backtracked state can be shortened by nucleolytic cleavage of the RNA to restore a properly aligned 3'-end in the active site. If backtracking persists, pol II requires the cleavage activity of the protein TFIIS to resume elongation (Fig. 1.4) [11] (TFIIS will be discussed in more detail below).

Pol II fidelity

The vast majority of enzymes either have a wide range of substrate specificity, which enables processing of structurally similar molecules, or a stringent requirement for a single substrate that is selected from a number of close homologs. Both RNA and DNA polymerases (DNA pol) are extraordinary, because they combine these features using a DNA template to change their substrate specificity after each round of catalysis [17]. Fidelity of DNA/RNA synthesis can be thought of as having two elements. The first relates to the selection of the correct (d)NTP from those not dictated by the DNA template (selectivity). The second reflects the ability to excise a misincorporated or incorrect nt after phosphodiester bond formation (proofreading). First, I will describe what is known about the fidelity of pol II and then make comparisons to DNA pol and other RNA pols.

Several studies *in vitro* with pol II determined that the maximal rate of polymerization (V_{max}) is reduced 500 to 10,000 fold for insertion of an incorrect

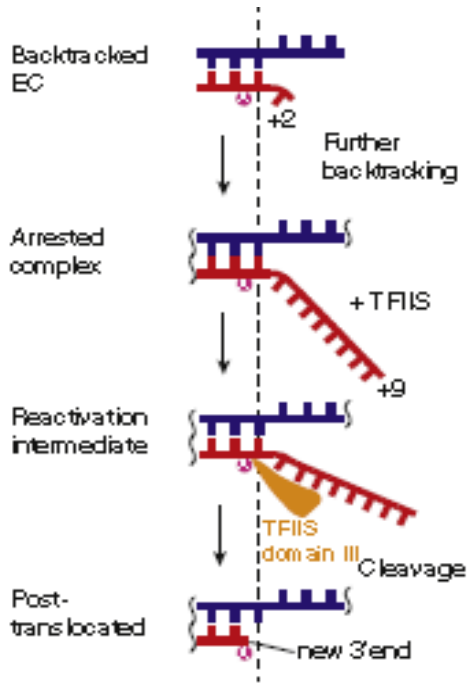

Fig. 1.4. Backtracking-RNA with a matched 3'-end. The dashed line represents the location of the insertion site relative to the DNA/RNA hybrid. The pink circle indicates the position of the active site. (modified from Cramer, P Biochimica et Biophysica Acta 1829 (2013) 9–19.)

nucleotide, depending upon the type of assay and sequence context, when compared to the rate for correct incorporation [18-21]. Additionally, the rate of correct nucleotide incorporation beyond a mismatch is reduced 20 fold [18]. The trigger loop (TL) of pol II has been identified as a critical feature of pol II that helps to ensure selection of the correct NTP [22] and will be more thoroughly discussed later.

Watson-Crick base-pairing provides the basis for selectivity. A study by Kellinger, *et al.* [23] uncovered the importance of complementary hydrogen bonding on the rate of catalysis, which was not obviously predictable. This was accomplished by exchanging the DNA base thymine with non-polar analogues deficient for hydrogen bonding. The lack of hydrogen bonding resulted in an increase in K_M by approximately 6 fold, but, incredibly, a decrease in the maximal rate of ATP incorporation by approximately 5000 fold. These findings implicate Watson-Crick base pairing as playing more than just a role in binding, but also in positioning the NTP for effective catalysis. Sydow, J. F. *et al.* [21] explored the foundation of selectivity by performing a systematic evaluation of all 16 incorporation possibilities, 12 of which are misincorporations. They found that overall transitions occurred slightly more efficiently than transversions. Furthermore, mismatches in the context of pyrimidine/pyrimidine (DNA nt/RNA nt) are formed more efficiently than purine/purine mismatches except in the case of C/C. On the other hand, purine/pyrimidine and pyrimidine/purine combinations both gave high and low efficiencies [21]. These varying results could be due to contaminating "correct" NTP in the nucleotides used in misincorporation experiments. Evidence of mismatch formation at the 3'-end of the RNA was not provided in these experiments. For example, a solution containing 1mM NTP (a concentration typical of a misincorporation experiment) with 99.9% purity could have a 1 µM contaminating NTP, which would be a significant concern because the K_M for correct nt extension has been estimated to be between 10 µM-100µM [18, 20, 23]. Taking into account the V_{MAX} and K_M for correct NTP extension determined by rapid-quench kinetics, it is possible to estimate what affect a NTP could have if it were the "correct" and contaminating NTP in a misincorporation experiment. A concentration of 1µM would result in a contribution to the observed rate

of about 65 min^{-1} whereas 10 nM would result in 0.66 min^{-1}. The typical rates reported for pol II misincorporation are around 1 min^{-1}, which emphasizes the effects contaminating "correct" NTP could have on the rates measured for misincorporation reactions. In addition, rates of correct nt incorporation, which were used for comparison to misincorporation rates, were assumed to have a linear dependence on NTP concentration over a 2000-fold change in NTP concentration without taking into consideration the K_M.

Interestingly, another study using *T. thermophilus* has suggested a template misalignment mechanism as an alternative model for generation of a RNA with a mismatched 3'-end, which is proposed to be applicable to pol II and all other multi-subunit RNA polymerases. In this model, the most likely incorporation, other than the correct nucleotide, corresponds to the nt specified by the next template DNA nt immediately downstream of the templating nt . This occurs when the templating base flips out of position allowing the next template nt to direct the addition of NTP to the 3'-end of the RNA [24]. In a subsequent study, it was demonstrated that pol II misincorporation is not dependent on the identity of the next templating nt, which is in disagreement with this model. [20].

Recently, higher resolution EC structures containing a preformed mismatch T/U (DNA nt/RNA nt) wobble base-pair, used to simulate a misincorporation, uncovered what has been termed the fraying site. The T/U base-pair is characterized by a shift in uridine and its 5'-phosphate away from the active site, when compared to a structure containing the matched T/A base-pair, along with loss of the active site Mg^{2+} (metal A) [21]. Two such fraying sites were observed in the context of the T/U mismatch when either an A/U or C/G bp was added to the RNA 3'-end to simulate a mismatch extension. In both structures the T/U mismatch was positioned as described before, however, the uridine was not base-paired with the template adenosine and flipped away from the template in a manner parallel to RNA/DNA hybrid axis. In the other structure the cytidine was also not base-paired with template guanosine, but in this case it occupied a different space perpendicular to the RNA/DNA hybrid. The distortion caused by the

addition of the incorrect nt to the 3'-end of an RNA should be emphasized, because it likely results in a paused state which could be followed by backtracking one nt from the mismatched, frayed site. This backwards movement of pol II, relative to the DNA template, then shifts the 3'-end of the RNA from the fraying site to the proofreading site (P-site) for nucleolytic removal of a dinucleotide (Fig. 1.5) [12]. The P-site is described in more detail below.

Initially, DNA pol was shown to utilize an intrinsic nucleolytic activity to remove damaged or misincorporated nt [25]. Later, transcriptional proofreading was demonstrated for RNA polymerase in *Escherichia coli*, where GreA protein associates with RNA polymerase and improves fidelity by enhancing removal of misincorporated nucleotides [26]. In *T. aquaticus* RNA polymerase, it was shown that the 3' end of the nascent RNA stimulates phosphodiester bond cleavage, providing active groups and coordination bonds to the active site, and this cleavage is enhanced for misincorporated nucleotides [27]. Pol I and Pol III have both been shown to have a strong intrinsic cleavage activity suggested to be important for proofreading [28, 29]. Whereas in archaea (*Methanococcus*), the TFS protein stimulates the intrinsic cleavage activity of RNA polymerase reducing the incorporation of "wrong" nt 700 fold [30]. Several studies have indicated that pol II does possess an inherent cleavage activity, and it is enhanced by the transcription factor TFIIS, which will be addressed in the following section [24, 31, 32].

It is intuitive that DNA pol would have a high level of fidelity because it must maintain the original genetic information of the cell, so it would be informative to compare DNA pol and pol II. They are similar in that both DNA pol and pol II have mobile structural elements referred to as the fingers domain and TL, respectively. The movement of these structures corresponds to "open" and "closed" forms of the enzyme, where the closed form is hypothesized to select for and promote catalysis of the template specified nt. Remarkably, the cleavage activity of DNA pol is performed in a separate domain that does not non-overlap with the domain that catalyzes phosphodiester bond formation, whereas, pol II performs these functions in a single domain [10, 33]. They

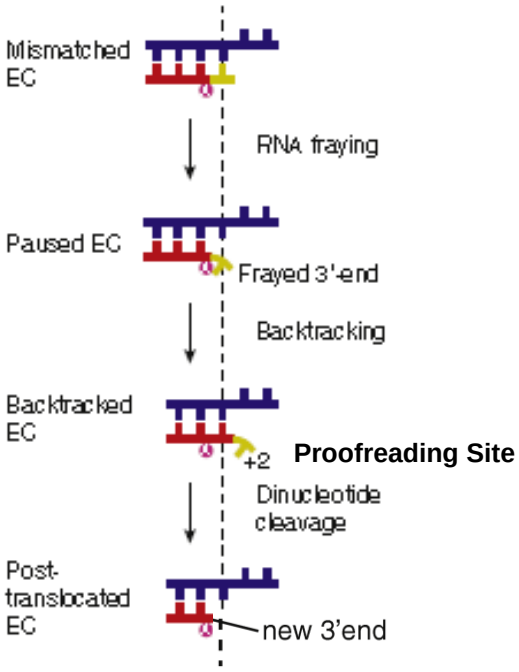

Fig. 1.5. Backtracking-RNA with a mismatched 3'-end. The dashed line represents the location of the insertion site relative to the DNA/RNA hybrid. The pink circle indicates the position of the active site. (modified from Cramer, P Biochimica et Biophysica Acta 1829 (2013) 9–19.)

also can be differentiated by the level of fidelity they can achieve. *In vitro* studies of T7 DNA pol reveal one error in 10^5 to 10^6 nucleotides incorporated. Conversely, for pol II the ability to select for the correct nt is much lower, one mistake in approximately 10^4 nt synthesized. T7 DNA pol fails to remove only one out of 10^3 to 10^4 base pairs mismatched, whereas for pol II this is estimated to be approximately 10^2. Combining the selectivity and proofreading components of fidelity gives an overall error frequency of 10^8 to 10^{10} for T7 DNA pol and 10^6 for pol II [17, 22]. Pol III has a similar *in vitro* error frequency of 10^6 as estimated from measurements using non-saturating concentrations of NTP, but this may underestimate the contribution of the selectivity component to fidelity [28]. Finally, *T. aquaticus* selects for the incorrect NTP every 10^4-10^5 nt [34].

The discrepancy in error frequency between DNA polymerases and RNA polymerases, however, does not diminish the importance of accurately transcribed genes. For example, Alzheimer's disease has been linked to molecular misreading, a phenomenon where transcriptional error leads to frameshift mutations, and aberrant neuronal proteins that accumulate and aggregate over time. Subsequently, it was also shown that these errors are not limited to neuronal tissue and contribute to non-neuronal age related diseases [35, 36].

A number of studies [18, 27, 28] have suggested a kinetic model for substrate selectivity and RNA proofreading by RNA polymerase (Fig. 1.6). In this model, n-1 represents an elongation complex with nascent RNA n-1 nucleotides in length whose 3'-terminal bases are completely complementary to the template. Extension of this RNA can follow two alternative paths. In one path, template-specified (correct, matched) NTPs can be added to the growing chain to generate ECs with RNAs containing n and then n+1 nucleotides, resulting in accurate transcription of the genetic information in the DNA template. Alternatively, an incorrect (mismatched) NTP can be added to generate an EC with a RNA whose 3'-end is not complementary to the template (n*). The partitioning of n-1 to products n and n* reflects the selectivity component of fidelity. Once an error has been generated by formation of n*, there are again two alternative paths, which reflect the proofreading component of fidelity. The RNA containing the

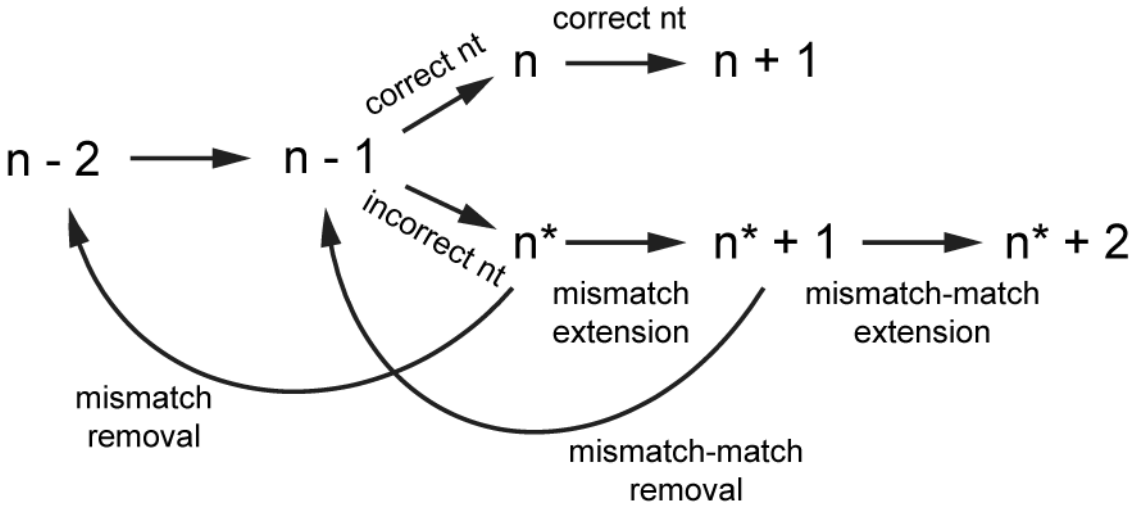

Fig. 1.6. Model for transcriptional fidelity. The schematic illustrates the roles of substrate selectivity and proofreading in transcriptional fidelity. See text for details.

mismatch can be extended to n*+1, propagating the error, or the mismatched NMP can be eliminated through cleavage of the RNA, which, in most cases, occurs between the n-2 and n-1 NMPs for a mismatch at n*. Cleavage generates a new, template-matched 3'-end at n-2 [37], which provides a substrate for restarting accurate transcription. If the mismatch is extended to n*+1, I show in Chapter 4 that proofreading can also occur at this position via cleavage between the n-1 and n NMPs.

TFIIS and backtracking

Pol II possesses an inherent nuclease activity, but it is substantially improved by the transcription cleavage factor TFIIS [18]. TFIIS is a 310 amino acid protein encoded by the gene *DST1* and is comprised of three domains (I, II, III) [38]. Domain I is not required for activity, but II and III, which consist of a three-helix bundle and zinc ribbon fold, respectively, are essential [39].

Crystal structures of backtracked EC bound to TFIIS have been enlightening. Domain II of TFIIS binds to the exterior of pol II via Rpb1. When TFIIS binds pol II, a conformational change occurs to widen the secondary channel. Domain III is then inserted into the secondary channel placing its β-hairpin in proximity to the active site. To facilitate cleavage, it is thought that the β-hairpin positions two of its acidic residues, (D290 and E291 in *S. cerevisiae*), to coordinate the transiently bound active site Mg^{2+}. This in turn aids in deprotonation of a water molecule for nucleophilic attack on the scissile phosphate [12, 15].

Deletion of *DST1* has very little measureable effect in some *in vivo* assays designed to assess fidelity [40, 41], but easily detectable effects have been seen in others [42]. These differences may reflect differential sensitivities of the assays, or, perhaps, that the indirect readout these assays provide is, at least in some cases, more sensitive to parameters other than transcriptional fidelity. It is clear, however, that intrinsic and TFIIS-mediated cleavage activities are important *in vivo*. TFIIS with alanine substitutions at D290 and E291 not only lacks the ability to stimulate cleavage, but it also inhibits intrinsic cleavage activity *in vitro* and, when overexpressed, confers a

severe growth defect when it is the only TFIIS present in yeast [43]. TFIIS, as well as its bacterial counterpart GreA, can stimulate removal of misincorporated NTPs *in vitro*, consistent with a possible role in proofreading [18, 44, 45]. However, the importance of TFIIS for fidelity has not been demonstrated *in vivo* under normal growth conditions [42, 46].

When pol II is backtracked one nt, the 3'-end of the RNA is misaligned with the active site and displaced to a defined P-site, which was mentioned earlier in the context of the fraying site. In this structure the β-hairpin tip of TFIIS overlaps with the P-site. The P-site effectively traps the one-nt backtracked EC to allow for sufficient time to cleave. The P-site stabilizes the positioning of the penultimate phosphodiester bond in the active site, which facilitates dinucleotide removal from the 3'-end of the RNA. If excision does not take place, further backtracking can occur. Binding sites for backtracking beyond the P-site have not been well defined except when the backtrack is greater than 7 nt. In structures with an RNA 3'-end extruded more than 7 nt, the RNA is clearly bound in the secondary channel extending to the entrance of the funnel. The "backtracking site" is consistent with an arrested complex. Upon TFIIS binding, the extruded RNA is displaced to a non-overlapping site termed the "restricted pore" [47, 48]. In these ECs, TFIIS is required to reactivate pol II and yields a corroborating 8-9nt cleavage fragment. See Fig. 1.7 for a model that integrates proposed mechanisms of the nucleotide addition cycle (NAC), backtracking, and proofreading.

Trigger loop and bridge helix

The TL and bridge helix (BH) are two critical structural features of the active center. They are both highly conserved in all multi-subunit polymerases, which implies a common mechanism of NTP addition for such polymerases. In fact, there is substantial evidence that suggests they function as movable elements important for NTP selection and alignment, phosphodiester bond formation and translocation [12, 22].

The BH is a 35 amino-acid (Rpb1 815-845) long α-helix that is positioned just downstream of the RNA hybrid and traverses the Rpb1/Rpb2 cleft. It is thought to be

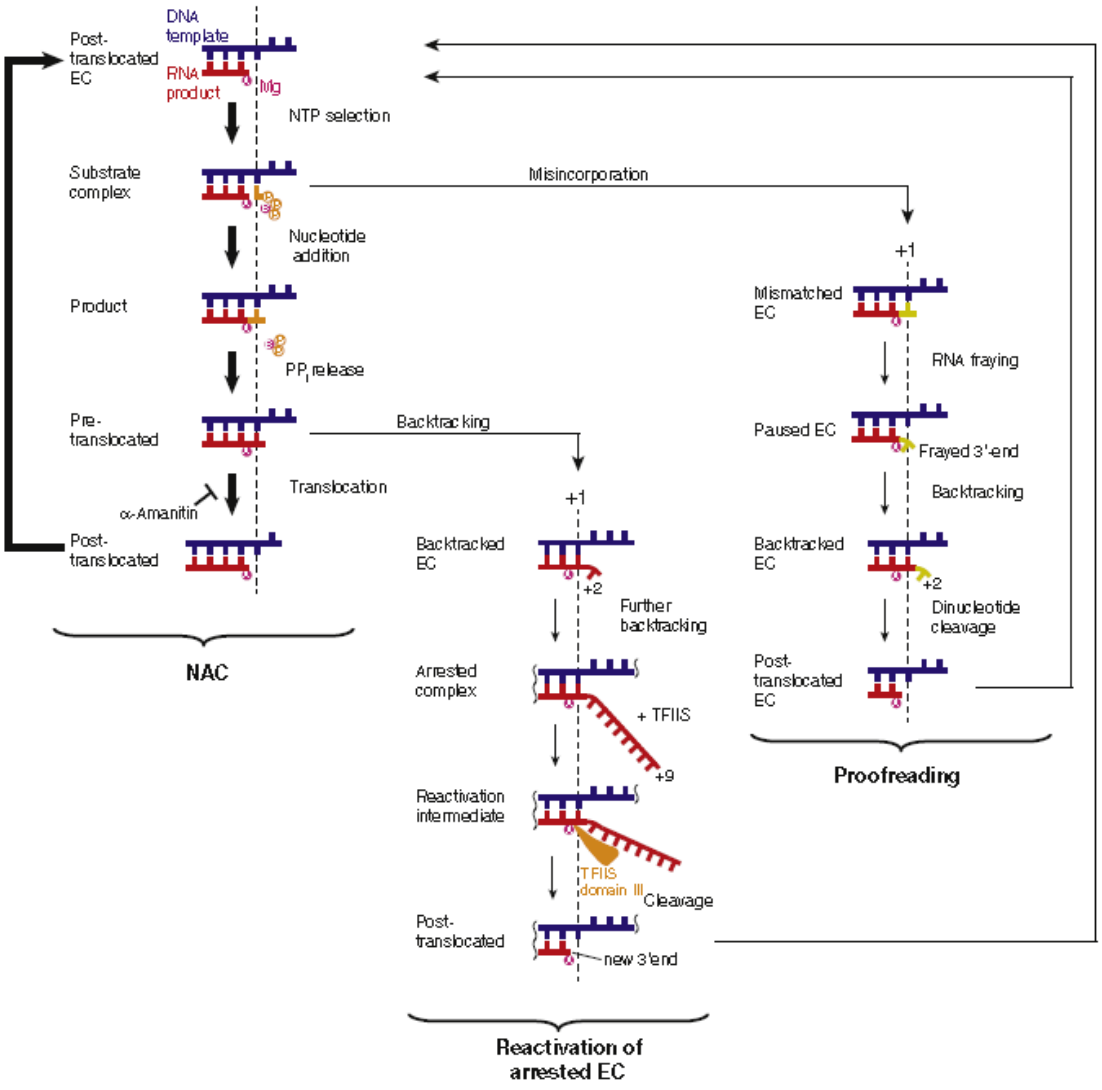

Fig. 1.7. Interconnecting models for NAC, backtracking, and proofreading. (modified from Cramer, P Biochimica et Biophysica Acta 1829 (2013) 9–19.)

involved in translocation, specifically by making and breaking contact with the coding nt. This idea originally materialized from comparing “bent” (towards the RNA hybrid) and “straight” BH structures observed in bacteria (bent and straight) and yeast (straight). These observations led to the hypothesis that the BH limits the movement of pol II to one nt, relative to DNA. Biochemical and mutational studies demonst ' BH ability to affect the transcription rate and fidelity of pol II [10-12].

The TL consists of approximately 35 amino-acids (Rpb1 1070-1105), and it is positioned next to the funnel and pore. Its folded conformation was first observed in crystal structures that had been soaked with the correct, but non-hydrolysable, NTP (GMPCPP) [49]. The TL is a highly flexible structure believed to have two essential conformations that reside in equilibrium. In the “open” conformation the TL is an unstructured loop positioned approximately 30 angstroms away from the active site [22]. In the “closed” conformation the TL forms an α-helical hairpin and swings toward the active center to make contact with the NTP in the insertion site [11]. The TL is thought to work like a trap door over the active center to bl he secondary channel entrance and provide functional groups that capture and position the correct nt for catalysis. The equilibrium shifts from an open “inactive” conformation in the absence of NTP base-paired to template DNA, to a closed “active” conformation upon binding of the correct NTP, this binding presumably then stabilizes the posttranslocated state. There is contention about the exact roles the TL plays in transcription, but its importance is clear, as demonstrated by a 60,000 fold decrease in transcription rate when it is omitted from *T. aquaticus* RNA polymerase [22].

The TL has also been proposed to be a key player in backtracking and translocation, and to work in concert with the BH. As discussed earlier, when the TL is closed, the secondary channel is obstructed. In this closed position the TL is located in the same space that is occupied by the RNA 3'-end in the backtracked conformation. In this way, the closed TL inhibits backtracking and possibly promotes forward translocation while the BH limits forward movement [50]. Intriguingly, when pol II was bound by TFIIS,

the TL was captured in a novel partially folded or open conformation referred to as the "locked" position, enabling access of the TFIIS acidic residues to the active site [48].

Mutational analysis of TL residues has provided some detail to the mechanism of pol II transcription. H1085 was identified as a potential proton donor to the pyrophosphate leaving group [49]. Mutation of this residue to tyrosine results in a slow, inaccurate pol II *in vitro* and a severe growth phenotype. However, it cannot be the primary catalytic residue because it does not account for the extreme defect of a complete TL deletion.

Interestingly, H1085 plays a central role in transcriptional inhibition induced by the pol II-specific toxin, α-amanitin [19]. It was first suggested from the crystal structure of pol II bound to α-amanitin [51], and supported later by kinetic studies [52], that the inhibitory effects on transcription arise from a blockage in translocation via the BH. Indeed, α-amanitin binds the funnel and pore just under the active site adjacent to the BH and TL. However, the single residue bound to α-amanitin was in a region of the BH that does not undergo movement. Further refinement of the pol II/α-amanitin complex led to the discovery that α-amanitin directly interacts with the TL through one of its mobile residues, H1085. Transcription experiments *in vitro* substantiated the requirement of H1085 for α-amanitin inhibition utilizing H1085Y. H1085Y was shown to be resistant to α-amanitin in several assays measuring NTP incorporation and TFIIS-mediated cleavage in "backtracked" ECs. It was reasoned from these findings that α-amanitin restricts TL movement solely through H1085, which is further supported by a lack of resistance shown in neighboring TL residues. Lastly, elongation rates measured in the presence of α-amanitin varied and were affected by the type of substrate used, suggesting that α-amanitin may impede catalysis in addition to translocation, or at the very least, that the translocation effects are substrate- specific [19]. A novel TL structure, termed the 'wedged' conformation, was observed in an EC with α-amanitin and is proposed to represent a translocation intermediate [50]. Fig. 1.8 relates a model for the NAC in the context of TL movement and α-amanitin inhibition.

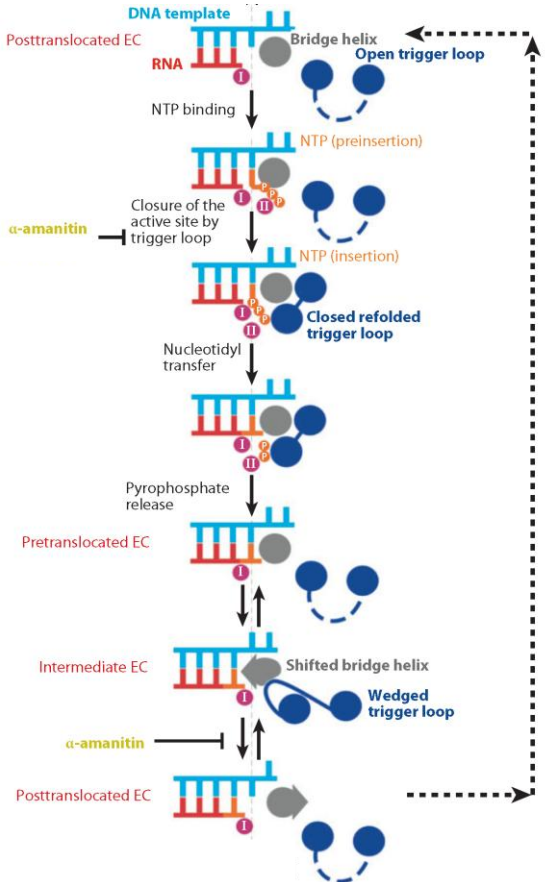

Fig. 1.8. NAC in the context of TL movement and α-amanitin inhibition. Circles with Roman numerals I and II represent metal A and metal B, respectively. (modified from Nudler, E. Annu. Rev. Biochem. 2009. 78:335–61).

E1103 is located close to the C-terminal pivot point of the TL. Its relevance was indicated by the point mutation E1103G, which was isolated because it displayed a synthetic lethal phenotype when combined with a *DST1* deletion [53]. An *in vivo* fidelity assay based on retrotransposition resulted in a 3-fold decrease in fidelity of E1103G when compared to pol II. *In vitro* E1103G is faster than pol II when incorporating either correct or incorrect substrates, which is possibly a consequence of a shift in equilibrium between the TL conformations to the closed form. The idea is that the faster rate of synthesis by E1103G arises from increased contact of the TL with substrate, which in turn promotes catalysis. This mutant decreases the fidelity of pol II, because the rate of misincorporation exceeds the pol II rate to a greater extent than the corresponding correct rates, which points to a defect in substrate discrimination [53]. Recent single molecule investigations further illustrate the significance of the TL by providing evidence that E1103 and H1085 affect NTP binding, phosphodiester bond formation, and translocation [54].

Rpb9

Rpb9 (122 amino acids) is a small, nonessential, subunit of pol II. As suggested by the high level of homology among eukaryotic pol IIs, the human homolog of Rpb9 can complement the growth defects observed in yeast cells lacking Rpb9 [6]. Strains with a deletion of the gene encoding Rpb9 (*rpb9*Δ) display hot and cold temperature sensitivity, and a slow growth phenotype at optimal temperature [40, 55, 56] in some but not in all genetic backgrounds [46]. Cells lacking Rpb9 are also sensitive to 6-azauracil and mycophenolic acid [56]. These compounds interfere with nt synthesis and have been shown to affect gene expression in vivo. Several mutants hypersensitive to these drugs cause altered start site selection of the IMD2 gene, involved in nt synthesis [57]. Moreover, start site selection determined for a handful of genes in the absence of Rpb9 results in a shift of initiation to alternative upstream sites [58, 59]. There is also evidence that suggests that Rpb9 is important in transcription coupled repair (TCR), a subpathway of nucleotide excision repair (NER) that specifically repairs damaged DNA template

within actively transcribed genes [60]. It was later proposed that the role of Rpb9 in TCR stems from its involvement in transcription elongation [61]. To date, 19 different genes have been identified to confer a synthetic lethal phenotype when deleted in combination with *rpb9*Δ (Table 1.1.). A synthetic lethal phenotype suggests that the proteins expressed by these genes may compensate for the loss of Rpb9 function or Rpb9 mediated functions. Some of these genes include members of large multi-protein complexes involved in transcription initiation, elongation, and chromatin modifications.

Rpb9 is located strategically at the front end of transcribing pol II, making contacts with Rpb1, Rpb2, and perhaps interacting with downstream DNA duplex (see Fig. 1.1). It forms part of the primary channel and extends near the surface of the enzyme to the secondary channel [7, 62]. Rpb9 consists of a N-terminal zinc ribbon fold (Zn1), C-terminal zinc ribbon fold (Zn2), and a central linker (Fig. 1.9). Part of the central linker forms a β-addition motif with β28 on the jaw structure of Rpb1, whereas Zn2 contacts the funnel structure of Rpb1. Both Zn1 and Zn2 interact with the lobe structure of Rpb2, except they are situated on opposite sides [63].

Inconsistent results have been reported when trying to relate the structure of Rpb9 to its function. Hemming, S. A. *et al.* [63] used GST-Rpb9 fusions to identify several alanine substitution mutations in Zn2 that hindered pol II recognition of pause and arrest sites, as well as response to TFIIS-induced cleavage activity at these sites *in vitro*, while multiple alanine substitutions in Zn1 behaved like pol II in these assays. Bacterially expressed Rpb9 highly aggregates in solution, but addition of a glutathione-S-transferase (GST) tag to Rpb9 results in a stable dimer, with dimerization likely occurring between GST-tags. This dimerization could be problematic, but GST-Rpb9 was shown to restore function to pol IIΔ9 in the assays tested [63, 64]. On the other hand, *in vivo*, a complete N-terminal domain was sufficient to complement growth and drug hypersensitivity phenotypes associated with *rpb9Δ* cells [58, 65], except in the case of menadione, which induces oxidative stress [46]. Moreover, alanine substitutions of Zn2 displayed no defects in start site selection or growth *in vivo* [56], which conflicts with an earlier study that identified the last 16 amino acids of the C-terminus as necessary for correct start site

GENE	Function
ADA2	subunit of SAGA and ADA complexes [65]
TAF9	subunit SAGA complexes and TFIID [66]
GCN5	subunit of SAGA [65]
NGG1	subunit of SAGA [65]
SPT3	subunit of SAGA [65]
SPT7	subunit of SAGA [67]
BRE1	E3 Ubiquitin ligase [68]
RAD6	ubiquitin conjugating enzyme [68]
ELP3	subunit of elongator complex [68]
SOH1	subunit of mediator complex [69]
GIM5	microtubule synthesis [69]
HTZ1	histone H2AZ variant [69]
LGE1	molecular function unknown [68]
NAB2	nuclear mRNA export and poly(A) tail length control [70]
RAD7	protein that recognizes and binds damaged DNA during NER [71]
RNA14	component of the cleavage and polyadenylation factor I (CF I) [72]
RPB4	pol II subunit [67]
RTR1	CTD phosphatase [73]
TFA1	TFIIE large subunit, involved in recruitment of pol II to the promoter [65]

Table 1.1. List of synthetic lethal genes. Genes that when deleted are lethal in combination with a *rpb9*Δ.

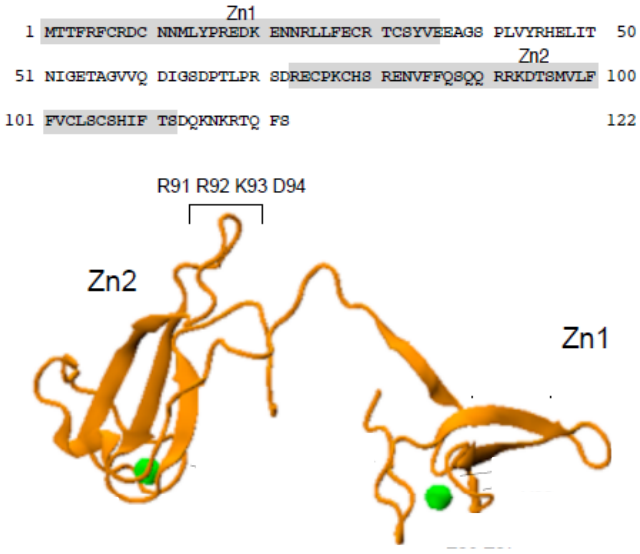

Fig. 1.9. Sequence and structure of Rpb9. Location of the zinc ribbon structures in the Rpb9 sequence and structure. The orientation of Rpb9 depicted here is similar to that shown in Fig1.1. Zinc atoms are represented as spheres.

selection [58]. To further complicate the role of Rpb9's domains, Zn2 of Rpb9 was shown to be essential for ubiquitylation and degradation of the Rpb1 subunit subsequent to UV damage of DNA [74]. It could be reasoned that the biologically relevant portion of Rpb9 consists of Zn1, but it is possible that the role Rpb9 plays in the observed growth defects may be separate from its other functions.

The zinc ribbons of Rpb9 share a great deal of homology with the A12.2 subunit of pol I and C11 subunit of pol III, which occupy positions analogous to that of Rpb9 in their respective polymerases. Unlike Rpb9, deletion of the gene encoding C11 is lethal. Both C11 and A12.2 are critical for intrinsic cleavage activity [29, 75, 76]. In light of this similarity, it is not surprising that the zinc ribbon of TFIIS shares 30% identity with the C-terminal domain of Rpb9, suggesting a role for Rpb9 in RNA cleavage activity [45, 63, 77]. Certainly, it has been shown in the context of defined pause and arrest sites that Rpb9 is important for TFIIS mediated cleavage. In the absence of Rpb9, pol II is more likely to transcribe beyond these sites and is less responsive to TFIIS mediated cleavage when these sites are recognized. Additionally, the cleavage products are different when compared to the cleavage patterns of pol II [31, 64]. Furthermore, in a recent publication a Rpb9-C11 hybrid with the C-terminal ribbon of Rpb9 replaced by that of C11 resulted in a significant increase in pol II intrinsic cleavage of a RNA with a mismatched 3'-end [78]. However striking these findings may be, they provide only indirect evidence of a role for Rpb9 in proofreading.

Rpb9 and transcriptional fidelity

Significantly, Rpb9 was shown in several studies to be important for fidelity. Deletion of *RPB9* increases expression of functional Can1 protein arising from a nonsense allele of *CAN1*, presumably due to transcription errors, and sequence analysis of cDNAs derived from an *rpb9*Δ strain provided direct evidence of increased base substitutions and insertions [40]. Increased expression of a functional protein from a plasmid-borne nonsense allele of *E. coli lacZ* in *rpb9*Δ yeast has also been observed [46]. Recently, a screen for revertants of *rpb9*Δ in the presence of menadione identified a

mutant allele of Rpb1 (G730D), which suppresses presumed *rpb9*Δ fidelity defects, as well as oxidative stress sensitivity [79].

In the following chapters I have endeavored to answer the following questions: How does Rpb9 contribute to fidelity? Is error-prone transcription intrinsic to Rpb9-deficient RNA polymerase II? What are the specific amino acids or regions of Rpb9 that promote accurate transcription?

CHAPTER II

MATERIALS AND METHODS

Yeast strains, growth, and preparation of whole cell extract

The parental *Saccharomyces cerevisiae* strain was derived from a protease deficient BJ5464 strain in which the *RPB3* ORF had been modified to contain two affinity tags, a 6X-His tag and a 26 amino acid sequence recognized by BirA, a bacterial biotin protein ligase [80]. This parental strain was generously provided by Mikhail Kashlev. The *RPB9* ORF was deleted from this strain (*rpb9*Δ*::kanMX4*) by PCR-mediated one-step gene disruption [81, 82]. Strains bearing expression vector (pRS416) with one or multiple point mutations of *RPB9* were constructed using PCR site-directed mutagenesis (Stratagene). Growth and manipulation of strains were done as described previously using standard protocols. Whole cell extract (WCE) was prepared as described by Kireeva, *et al.* [80].

Pol II and TFIIS purification

Pol II and pol IIΔ9 were purified essentially as described by Kireeva, *et al* .[80] with modifications described by Sydow, *et al.* [21]. The recombinant TFIIS used in assays with purified pol II was a cleavage competent N-terminal truncation of TFIIS (TFIIS Δ2-146) [19] and was generously provided by Craig Kaplan.

RNA labeling and RNA-DNA hybrid formation

RNA and DNA oligomers were purchased from Oligos Etc. (Wilsonville, OR) or Integrated DNA Technologies (Coralville, IA). RNA oligos (16.7 pmol) were labeled with [γ-^{32}P]ATP (16.7 pmol) (3000 Ci/mmol, Perkin Elmer cat# BLU002A) using T4 polynucleotide kinase (Promega cat# M4101) in transcription buffer TB(40) [20 mM Tris-HCl (pH 7.9), 40 mM KCl, 5 mM $MgCl_2$, 2 mM 2-mercaptoethanol]. It was then

annealed with the appropriate DNA template strand (16.7 pmol) as described by Kireeva, *et al.* [80]. Unlabeled NTPs were obtained from GE Healthcare.

Elongation complex assembly and *in vitro* transcription

Assembly of elongation complexes (ECs) was essentially as described by Kireeva, *et al.* [80]. Purified pol II or pol IIΔ9 (250 ng) or WCE (25 µL) was added to 25 µL of Ni^{2+}-NTA beads (Qiagen cat# 30210), that had been washed in TB(40). Binding and wash steps were performed at room temperature using an orbital shaker at 1000 rpm (VWR cat# 12620-930). After 30 min the beads were washed with 1 mL of TB(1000) (same composition as TB(40) except with 1M KCl) for 10 min and then washed 3 times with 1 mL of TB(40). RNA-DNA hybrid (1 pmol) was then incubated with the beads for 10 min in a total volume of 100-150 µL, followed by addition of the nontemplate DNA strand (10 pmol) for an additional 10 min. ECs were then washed with 1 mL of TB(1000) for 10 min and then three times 1 mL with TB(40). The final suspension of immobilized ECs was in 100-200 µL of TB(40). After addition of NTPs or TFIIS, aliquots (10 µL) were removed at various times and added to a tube containing 10 µL of 2X gel loading buffer [10 M urea, 50 mM EDTA (pH 7.9), 0.005% bromophenol blue, 0.005% xylene cyanol]. Samples were fractionated by polyacrylamide gel electrophoresis with a gel containing 20% acrylamide (19:1 acrylamide:bisacrylamide), 7 M urea, and TBE [50 mM Tris-borate (pH 8.3), 1 mM EDTA]. ECs with mismatched RNAs using WCE were assembled as above, except 10 min incubation times were shortened to 1 min to reduce the extent of cleavage during assembly. For assays using α-amanitin, ECs were assembled as described and incubated with 160 µg/mL α-amanitin (Calbiochem cat#129741) for 3 minutes before adding the appropriate NTPs. RNAs were visualized and quantitated with a Phosphorimager (Bio-Rad PharosFX Plus). First order fits were performed with Kaleidagraph software (Synergy Software, Reading, PA).

Western blotting

WCE preparations (100 µL-500 µL) were incubated with 10 µL Ni^{2+}-NTA beads for 30 minutes and washed exactly as done for EC assembly. Next, 20µL of 2X SDS gel loading dye (100 mM Tris-Cl pH 6.8, 200 mM dithiothreitol, 4% SDS, 0.2% bromophenol blue, 20% glycerol) was added. Samples were boiled for two minutes and loaded on to 4-20% SDS polyacrylamide gel (Biorad cat#345-0032) along with 10 µL fluorescent marker (Genescript cat# M00124). The proteins were then transferred overnight at room temperature (15V) to PVDF Sequi-blot membrane (Biorad cat#162-0186). The blot was then blocked with 3% non-fat dry milk in 1X TBS (100 mM Tris-Cl pH 7.5, 150 mM NaCl) for 1 hour followed by incubation at 4°C overnight with anti-Flag 1:1000 (Sigma cat# F1804) in 3% non-fat dry milk, 1X TBS. After washing the blot 5 times with 1X TBS, anti-mouse IgG 1:30,000 (Sigma cat#A9044) was added at room temperature for 30 min and was washed an additional 5 times with 1X TBS. The blot was then incubated with Supersignal West Femto substrate (Thermofisher Scientific cat# 34095) for 5 minutes and visualized using a chemiluminescent imager (Biorad ChemiDoc XRS). To compare the ratios of Rpb9 and mutant Rpb9 protein to the Rpb1 subunit, the blots were washed, re-blocked, and probed with anti-RNA pol II 8WG16 1:500 (Covance cat# MMS-126R) in 1X TBS at 4°C overnight followed by exposure and imaging as described above.

CHAPTER III

FIDELITY OF RNA POLYMERASE II TRANSCRIPTION: ROLE OF RBP9 IN NUCLEOTIDE DISCRIMINATION

Introduction

The accuracy of transcription is of clear importance in gene expression, as errors in transcription can result in proteins with altered function. The error frequency of eukaryotic RNA polymerase II (pol II) *in vitro* has been measured in a number of studies [12, 44, 83], and estimates vary between about 10^{-3} and 10^{-6} errors per nucleotide incorporated, depending on the template and the concentration and type of divalent metal ion present. Recent studies have suggested one mechanism by which pol II (as well as other multisubunit RNA polymerases) discriminate correct, template-specified NTPs from incorrect NTPs and dNTPs. This selectivity depends on the TL, a mobile structural element within Rpb1, the largest of the pol II subunits. The TL can move into proximity of the active site, a conformational change that serves to trap the correct NTP and position functional groups required for catalysis [19, 49, 53]. The role of the TL in transcription has been discussed in the introduction, as well as several recent reviews [10, 12, 22, 49, 84].

Rpb9 is a small (122 amino acids in *S. cerevisiae*) pol II subunit that is highly conserved among eukaryotes [77, 85]. Although Rpb9 is not essential for growth in yeast, *rpb9* null mutants have growth and drug hypersensitivity phenotypes [55, 67, 86], as well as upstream shifts in transcription start sites for a number of genes [59, 87, 88]. Several studies have suggested a role for Rpb9 in transcriptional fidelity. Deletion of *RPB9* was shown to increase expression of functional Can1 protein arising from a nonsense allele of *CAN1*, presumably due to transcription errors, and sequence analysis of cDNAs derived from an *rpb9*Δ strain provided direct evidence of increased base substitutions and insertions [40]. Increased expression of a functional protein from a

plasmid-borne nonsense allele of *E. coli lacZ* in *rpb9*Δ yeast has also been observed [46].

In this chapter, I demonstrate that, while the absence of Rpb9 increases the rate of misincorporation of ATP or UTP in a sequence context where CTP is specified by the DNA template, there are nearly identical increases in the rate of CTP incorporation resulting in little or no effect on selectivity. These results are not in accord with experiments published while my work was in progress, and I discuss possible reasons for the differences.

Results

Pol II derived from an *rpb9*Δ strain increases the rate of UTP for CTP errors

In order to study the role of Rpb9 in selectivity I used an *in vitro* assay that utilizes a promoter-independent template without the need for transcription factors [80]. This is possible because pol II can specifically bind to and initiate on artificially assembled transcription bubbles with template DNA hybridized to short RNA oligonucleotides. In initial, preliminary experiments, pol II was immobilized from whole cell extract (WCE) preparations derived from a strain of protease-deficient yeast with the Rpb3 subunit of pol II bearing a 6X histidine affinity tag. This same strain was used to generate a *rpb9Δ* strain in which the *RPB9* ORF was deleted (*rpb9*Δ*::kanMX4*) by PCR-mediated one-step gene disruption [81, 82]. First, either pol II or pol II from an *rpb9Δ* strain was immobilized on Ni^{2+}-NTA agarose beads, and after several washes to remove non-specific protein interactions with the beads, a preannealed hybrid consisting of a 5'-end ^{32}P labeled 10 nt RNA and a complementary 40 nt DNA template strand was added. This was followed by inclusion of a 40 nt DNA non-template strand to complete transcription bubble assembly (Fig. 3.1A). Again, the fact that the newly formed transcription EC was secured to a solid medium was exploited, and the ECs were washed to remove free and non-specifically bound nucleic acids. All of these steps were performed at room temperature.

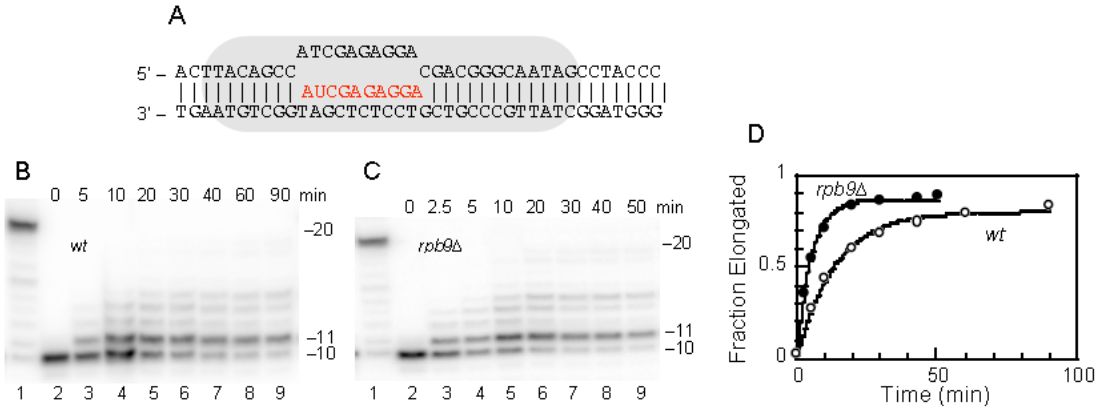

Fig. 3.1. Misincorporation of UTP for CTP. *A*. Elongation complex assembled from oligonucleotides. The template strand of DNA is on the bottom. Transcription extends the RNA oligo to the right beginning with CTP. The shaded area shows the approximate region associated with pol II. *B* and *C*. Elongation complexes as shown in A were incubated with ATP, CTP, and GTP (10 μM each) for 30 sec (lanes 1) or for the indicated times with UTP (1 mM). *B*. pol II derived from wild-type cells. *C*. pol II derived from *rpb9Δ* cells. *D*. Quantitation of results from B and C. The curves are first-order fits to the data.

Immediately after assembly, all of the labeled RNA is, as expected, in a single band of 10 nt (Fig. 3.1 B and C, lanes 2). Essentially all of this RNA was within a functional EC, as addition of ATP, GTP, and CTP (10 μM each) resulted in rapid elongation to 20 nt, where UTP is specified by the template (lanes 1). To extend the 10 nt RNA to 11 nt requires CTP as dictated by the template strand. However, to measure the rate of misincorporation, only UTP (1 mM) was added. Aliquots were removed and the reaction was quenched at various times to monitor the time course of mismatch formation (Fig 3.1B, C lanes 2-9). The products of the reaction were resolved on a 20% polyacrylamide gel, and quantified by phosphorimager analysis. It was assumed that bands larger than 11 nt were derived from misincorporations at 11 nt with U, and their combined intensities were added to the signal intensity of 11mer. Verification of mismatch formation will be discussed in detail in the following sections. The fraction of UTP misincorporation was plotted, and the data were fit to an exponential first-order equation (Fig. 3. 1D). Pol II immobilized from the *rpb9Δ* strain (closed circles) exhibited a rate of misincorporation that was approximately three times faster than that immobilized from the wild-type strain (open circles). The observed rate constants at this concentration of UTP were 0.194 min^{-1} (*rpb9Δ*) and 0.074 min^{-1} (wt). Experiments at different concentrations of UTP suggest that 1 mM is at or near a saturating concentration for misincorporation (data not shown). In additional experiments with the same template sequence, but using ATP as the misincorporation nt, the absence of Rpb9 also resulted in a faster rate of misincorporation (data not shown).

Purification of pol II

The WCE preparations used in these preliminary experiments contain proteins that could affect the observed misincorporation rate, and such proteins could associate with pol II in an Rpb9-dependent manner. To determine if the alterations in misincorporation rate are intrinsic to pol IIΔ9, I purified pol II and pol IIΔ9 to assay *in vitro* [80]. In addition to the Rpb3 6X Histidine tag utilized in the *in vitro* studies, this subunit contains a 26 amino acid insertion that provides a substrate for BirA, a bacterial biotin

protein ligase. The first step in the purification entails biotinylating the polymerase in the WCE, followed by binding to Ni^{2+}-NTA agarose and release with imidazole. The eluate is then bound to an avidin column where the polymerase is further purified and released with an excess of biotin. Fig. 3.2 represents purified pol II and pol IIΔ9 using this method. Purity was determined using sodium dodecyl-sulfate polyacrylamide gel electrophoresis (SDS-PAGE) followed by Coomassie or silver stain staining. This gel confirms the purity of the enzyme preparations, as well as the absence of the Rpb9 subunit in the strain that was characterized genetically as *rpb9*Δ. I also used an alternative purification method successfully, which utilized the 6X-Histidine tag of Rpb3, but was followed instead by ion-exchange [21] and gel filtration chromatography.

Absence of Rpb9 increases the rate of misincorporation

ECs were assembled using purified pol II to measure the rate of misincorporation using either an incorrect purine or pyrimidine base in place of the correct base CTP. UTP 1 mM (Fig. 3.3A) or ATP 1mM (Fig. 3.3C) was added to an EC bearing an RNA with a matched 3' end (10nt) using either pol II or pol IIΔ9. The box represents an abbreviated version of the EC portrayed in Fig. 3.1A and this representation will be used throughout the remainder of this document to highlight only the relevant portion of EC where changes in sequence are made. The complete template and non-template DNA are present in all ECs. The appearance of the extended RNA (11nt) was observed over a 2-3 hour period (Fig. 3.3A, C lanes 2-9 and 13-20, 2-8 and 12-18). The fraction of ECs extended to 11nt or greater was plotted versus time, and the data were fit to a single exponential equation to obtain k_{obs} (Fig. 3.3B, D). The UTP misincorporation rate for pol IIΔ9 (k_{obs} = 0.081 min^{-1}) was approximately three times faster than pol II (k_{obs} = 0.025 min^{-1}), and for ATP the rate for pol IIΔ9 (k_{obs} = 0.092 min^{-1}) was about two times faster than pol II (k_{obs} = 0.041 min^{-1}). It was determined that increasing the NTP concentration above 1 mM did not result in a significant increase in the rate of misincorporation, which indicated that 1 mM is a near saturating for both UTP and ATP (data not shown and Fig. 3.5A). These results demonstrate that the faster rate of misincorporation observed in the

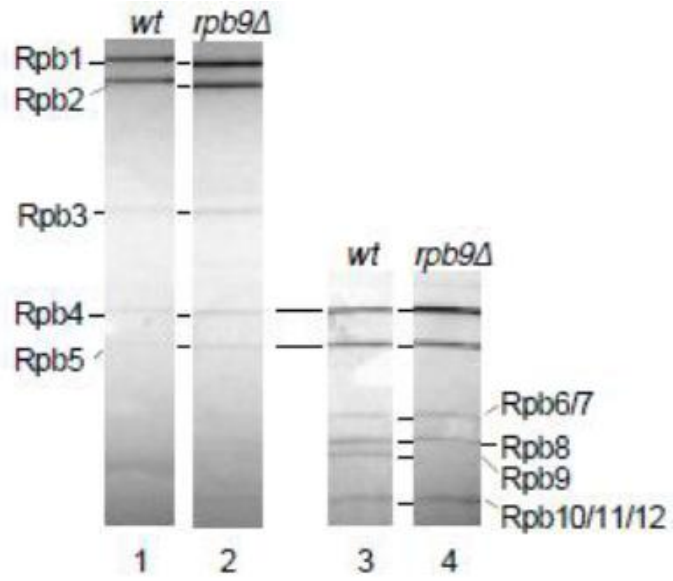

Fig. 3.2. SDS polyacrylamide gel electrophoresis of purified pol II. Lanes 1 and 2 were stained with Coomassie blue, lanes 3 and 4 were silver stained. Bands were identified from their size relative to a molecular weight marker resolved in an adjacent lane (not shown).

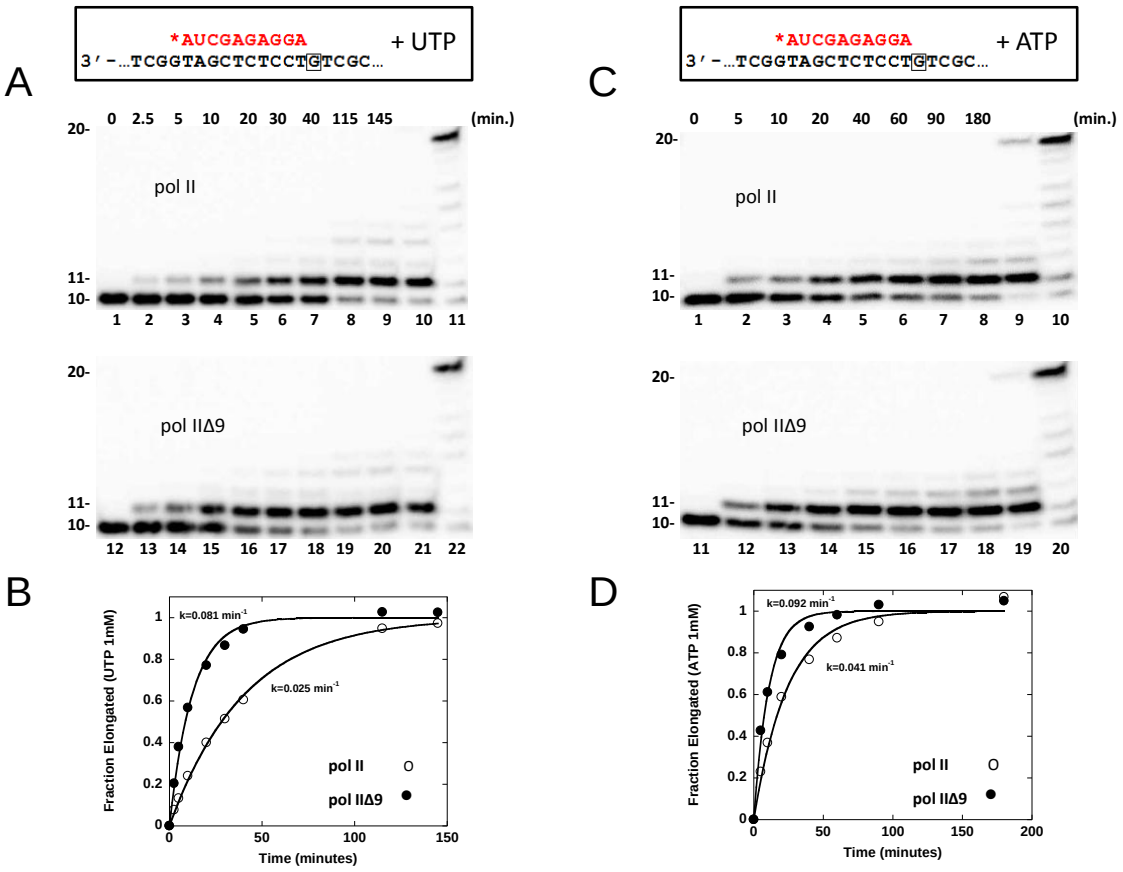

Fig. 3.3. Pol IIΔ9 increases the rate of NTP misicorporation. *A,C* The box shows the abbreviated form of the EC in Fig. 3.1C. and the small box identifies the template nt that designates the next correct nt at position (n), CTP. An incorrect nt, UTP 1 mM (lanes 2-9 and 13-20) or ATP 1 mM (lanes 2-8 and 11-18), was added to the EC formed with pol II or pol IIΔ9. *A*, lanes 10 and 21, and *C*, lanes 9 and 19 ECs were first exposed to UTP (1 mM) or ATP (1 mM) and then chased with A, C, G and U (10 μM) for 30s. *A*, lanes 11 and 22, and *C*, lanes 10 and 20 ECs exposed to A, C, G and U (10 μM) for 30s in the absence or UTP or ATP misincorporation. The experiment was repeated at least twice at this concentration for each NTP. Higher concentrations tested gave almost identical rates. *B, D* The fraction of EC that extended with UTP or ATP to 11 nt or greater was plotted and fit to a single exponential equation to obtain k_{obs}. Open circle represents pol II and closed circle pol IIΔ9. To emphasize the difference in rate between pol II and pol IIΔ9 the fraction elongated was divided by the extent of the reaction, as determined from the fit.

absence of Rpb9 is an inherent property of the polymerase and is not the result of differential association of accessory proteins in a Rpb9-dependent fashion.

For misincorporation experiments, it is critical to show that the extended 3'-end of the transcript actually contains a mismatch and is not the result of small amounts of contaminating NTP complementary to the template. In some studies it has been possible to distinguish a mismatched 3'-end by exploiting electrophoretic mobility differences between the matched and mismatched RNA products [18, 21]. In this study, I have taken an approach that exploits kinetic differences in pol II-mediated extension of matched and mismatched 3'-ends. The rate of correct nucleotide extension from a mismatched 3'-end has been reported to be at least 20x slower than from a matched end [18], and, as shown in Chapter 4, I have determined that, at least in the sequence contexts I have used, the rate difference is significantly larger than that. With this in mind, I added a low concentration of ATP, CTP, and GTP (10 μM) to the last time point taken and then stopped the reaction after 30s (Fig. 3.3A lanes 10 and 21, Fig. 3.3C 9 and 19); in each lane little if any of the 11-mer is extended by addition of these nucleotides, as would be expected for a mismatched 3'-end. However, under these same conditions, the 10-mer with a matched 3'-end is completely extended to 20 nt (Fig 3.3A lanes 11 and 22, and Fig. 3.3C lanes 10 and 20. The behavior of matched and mismatched 3'-ends is best seen in Fig. 3.3C (compare lanes 8 and 9), where, after the addition of NTPs, the small amount of remaining 10-mer is rapidly extended to 20 nt, while the 11-mer is not extended.

Absence of Rpb9 increases the rate of elongation with the correct nucleotide

To test the effect of Rpb9 on selectivity it was necessary to also measure the rate of elongation with "correct" NTPs that are specified by the template. This can be problematic, as these rates are very rapid at NTP concentrations comparable to those present in vivo [89]. Some studies have directly determined the correct rate of single nucleotide incorporation using rapid quench-flow kinetics [20]. Others have estimated the average rate of elongation across relatively long DNA templates where the rate was

calculated by dividing the number of nt synthesized by the halftime of extension [19]. I have used this second method. I assembled EC *in vitro* using purified pol II and pol IIΔ9 [80] as shown in Fig. 3.4C, and simultaneously added all four nucleoside triphosphates (NTP) ATP, CTP, GTP, and UTP and monitored transcription over time for pol II and pol IIΔ9 (Fig. 3.4A, B). I determined the halftime for the appearance of products >60 nt in length at four different concentrations of NTPs. The average rate of elongation was calculated by dividing the actual number of nt synthesized (52 nt) by the half time. These rates were then plotted against their respective concentrations, and the curve was fit to the Michaelis-Menton equation (Fig. 3.4D). These data revealed approximately a two-fold difference in the maximal rates of elongation of pol II and pol IIΔ9 (5.4±0.24 nt s^{-1} and 13±0.58 nt s^{-1} respectively). The apparent K_M for pol II and pol IIΔ9 were 85±16 μM and 175±27 μM respectively. These parameters for the pol II are similar to those reported previously using this method [19]. In the next section I relate these data to misincorporation experiments to estimate selectivity.

Rpb9 and selectivity

Selectivity can be determined by dividing the catalytic efficiency (V_{max}/ K_M) for a "correct" nt incorporation by the catalytic efficiency of an "incorrect" nt incorporation. Results from the long-template assay (Fig. 3.4) allowed this parameter to be calculated for correct nt incorporation as an average of the different sequence contexts encountered during transcription of the long template (Fig. 3.5C). V_{max} and K_M for ATP misincorporation were determined by measuring the rate of misincorporation at several concentrations of ATP and fitting the results to the Michaelis-Menten equation (Fig. 3.5A). These results revealed no difference in selectivity when Rpb9 is absent from pol II (Fig. 3.5C).

This result conflicts with another study in which the absence of Rpb9 was reported to cause a 5-fold decrease in pol II selectivity [20]. In this study V_{max} and K_M for correct nt incorporation were determined by single nt addition. This approach has several advantages over the long template in that potential Rpb9 effects on pausing or

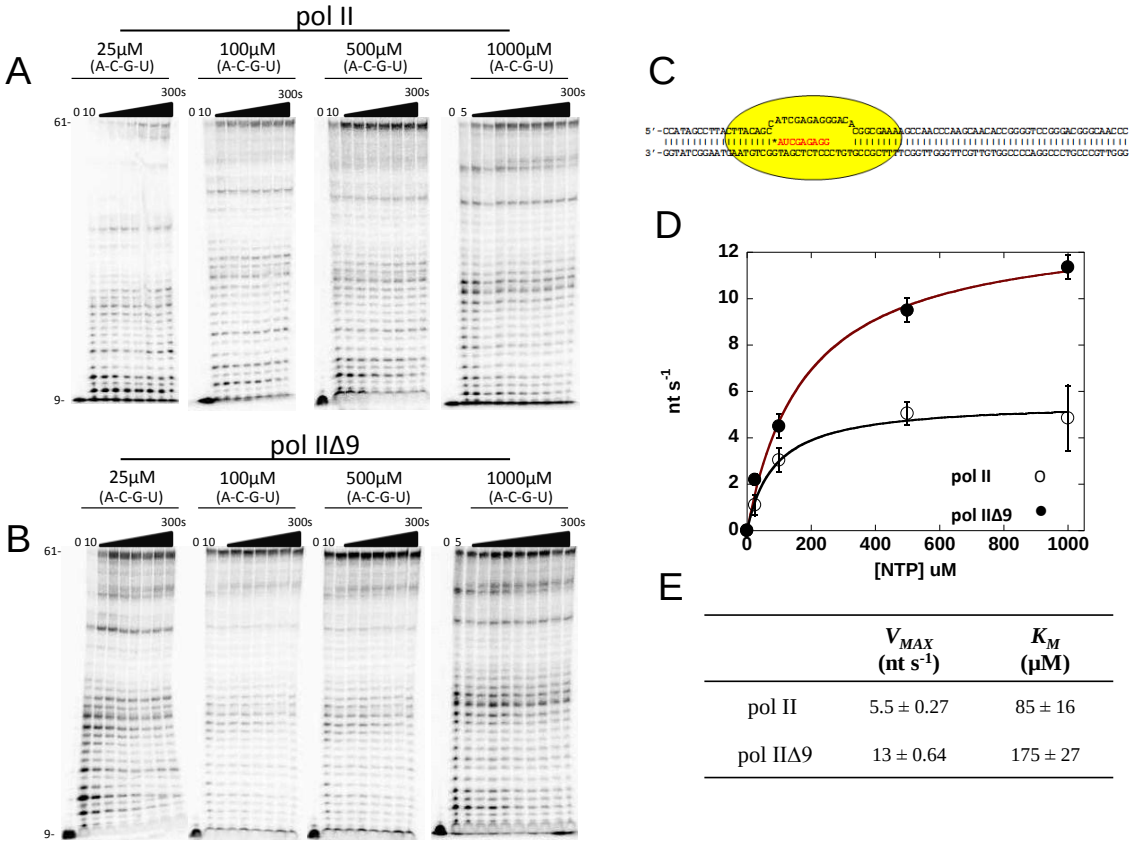

	V_{MAX} (nt s^{-1})	K_M (μM)
pol II	5.5 ± 0.27	85 ± 16
pol IIΔ9	13 ± 0.64	175 ± 27

Fig. 3.4. Pol IIΔ9 increases the rate of elongation. *A, B*, The average rate of elongation for pol II and pol IIΔ9 was estimated by adding simultaneously ATP, CTP, GTP, and UTP to the EC shown in *C*. The concentration of each NTP added was 25, 100, 500, or 1000 μM. Each experiment was repeated three times to calculate standard deviation. The run-off product is indicated at 61 nt. The fraction of ECs that extended to >60 nt was plotted versus time for each concentration and the data were fit to a non-linear equation to determine the half time. The actual number of nt synthesized (51) were divided by the half time to determine the average rate of extension *D*, The rates calculated for *A* and *B* were plotted against their respective concentrations and fit to the Michaelis-Menton equation. Open circle represents pol II and closed circle pol IIΔ9. *E*, Summary of parameters derived from the fit to the Michaelis-Menten equation.

A

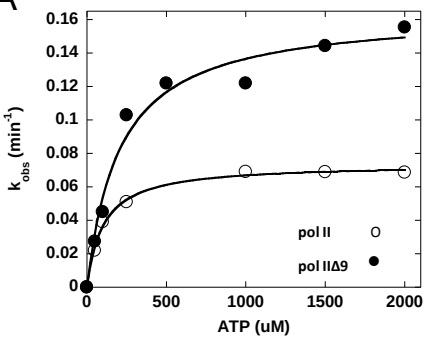

B

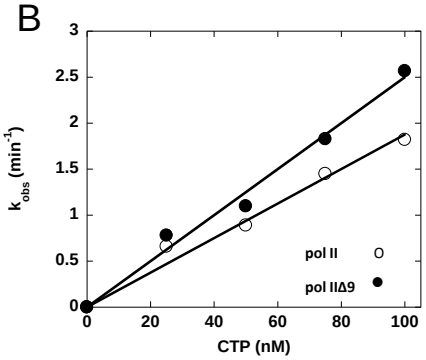

C

	NTP	V_{max} (s^{-1})	K_M (µM)	$Vmax/K_M$ (s^{-1} $µM^{-1}$)	Selectivity
pol II	ACGU (correct)	0.080 ± 0.003	85 ± 16	$9.5\times10^{-4} \pm 1.9\times10^{-4}$	79
	CTP (correct)	--	--	0.313	2.6×10^{4}
	ATP (incorrect)	$1.2\times10^{-3} \pm 2.3\times10^{-5}$	102 ± 9.3	$1.2\times10^{-5} \pm 2.5\times10^{-6}$	
pol IIΔ9	ACGU (correct)	0.18 ± 0.008	175 ± 27	$1.0\times10^{-3} \pm 3.0\times10^{-4}$	78
	CTP (correct)	--	--	0.416	3.2×10^{4}
	ATP (incorrect)	$2.7\times10^{-3} \pm 1.5\times10^{-4}$	206 ± 43	$1.3\times10^{-5} \pm 3.5\times10^{-6}$	

Fig. 3.5. NTP Selectivity. *A, B,* All the data in these plots were obtained using pol II and pol IIΔ9 assembled with ECs as shown in Fig. 3.3A. *A,* The plot shows rates of misincorporation measured at different concentrations of ATP. The data were fit to the Michaelis-Menten equation to extrapolate the parameters for V_{MAX} and K_M. *B.* The plot reflects rates of correct nt incorporation (CTP) at low concentrations. The slope of the line was used to estimate the V_{max}/K_M for this reaction. *C,* Summary of kinetic parameters obtained using the long template assay for correct incorporation rate (ACGU), misincorporation (ATP), and correct single nt addition (CTP) estimates.

backtracking are eliminated, and the same sequence context can be used to determine rates of correct and incorrect nt addition. However, the rapid rate of correct nt addition requires special instrumentation to measure. To partially circumvent this problem and allow comparison of correct and incorrect catalytic efficiencies in identical sequence contexts, I took advantage of the fact that at substrate concentrations well below K_M, the Michaelis-Menten equation reduces to a form in which a plot of rate versus substrate concentration yields a straight line with slope V_{max}/K_M. Using CTP concentrations at or below 100 nM, where the rates are easily measured without special instrumentation, V_{max}/K_M for correct CTP addition for both pol II and pol IIΔ9 could be measured directly (Fig. 3.5B) with the same ECs used to measure ATP misincorporation in Fig. 3.5A. The results are in general agreement with measurements made with rapid quench flow instruments [20]. However, no difference in selectivity between pol II and pol IIΔ9 was observed (Fig. 3.5C).

In the assays discussed so far, selectivity is determined from NTP incorporation where only the correct or incorrect NTP is available for RNA extension. However, it may be more relevant to determine selectivity in a situation that includes the potential for direct competition of the correct and incorrect NTP. To do this, I developed an assay based on studies to determine discrimination between rNTP and dNTP by *Escherichia coli* RNA polymerase [84]. Essentially, I reduced the concentration of the correct NTP, so that the rate of incorporation of this nt is comparable to the rate of inserting an incorrect nt. In this way, the occurrence of misincorporation is increased and any differences between pol II and pol IIΔ9 in nt discrimination could be readily observed. The experiment was designed to evaluate selectivity for correct CTP in the presence of a large excess of incorrect UTP.

The EC used along with the outline of the experimental design is depicted in Fig. 3.6A. ECs with a RNA 10 nt in length were incubated with 1 mM UTP and a low (0.5-16 nM) concentration of CTP. Elongation of one nt with either of these substrates generates an RNA of 11 nt. In order to distinguish 11-mers with matched (C) or mismatched (U) ends, a low concentration of GTP (1 μM), the nt complementary to the

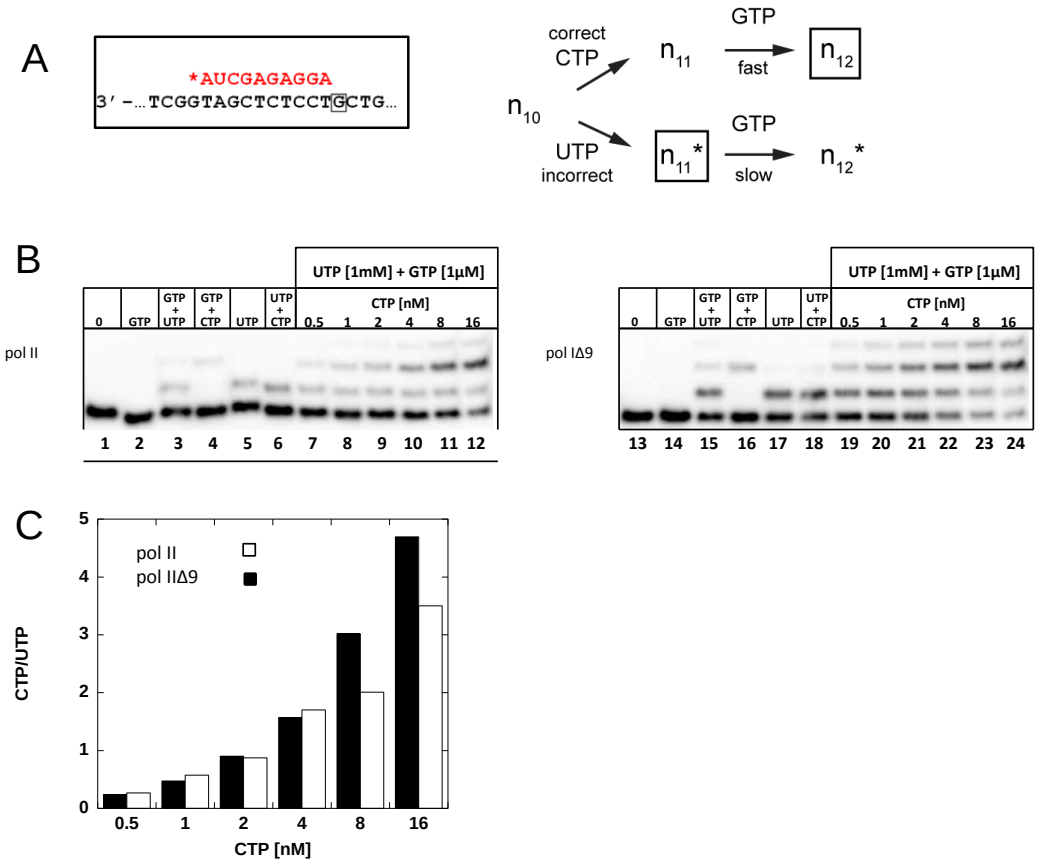

Fig. 3.6. Assay to determine selectivity by direct competition of CTP and UTP. *A*, The box shows the abbreviated form of the EC in Fig. 5.1C. and the small box identifies the template nt that designates the nt at position (n), CTP. *B*, The model describes the expected outcomes for either a correct nt or an incorrect extension. *C*, To each EC UTP (1 mM), GTP 1 μM) and a varying nanomolar concentration of CTP was added and extension was stopped after 10 minutes (lanes 7-12 and 19-24). For controls, extension was also stopped after 10 minutes, but contained a single nt or combinations of two out of the three nt that were added to experimental ECs to determine the fraction ECs that deviate from the expected outcomes outlined in the model. GTP only (1 μM) was used to estimate the fraction of ECs with a GTP misincorporation. GTP (1 μM) + UTP (1 mM) was used to estimate the fraction of ECs with a mismatched 3'-end extended with GTP. GTP (1 μM) + CTP (0.5 nM) was used to determine the fraction of ECs that rapidly extend to 12 nt with CTP and GTP. UTP (1 mM) was used to estimate the extent of UTP misincorporation beyond 11 nt. UTP (1 mM) + CTP (0.5 nM) was used to estimate the fraction of ECs that extend beyond 11 nt when UTP and CTP are added simultaneously (lanes 2-6 and 14-18). *D*, The graph reflects CTP/UTP ratios that were adjusted by subtraction of unexpected extension, which was determined in the above control reactions. This was done for each concentrations of CTP.

template at position 12, was also included. The matched-end 11-mer should very quickly be elongated to 12, while the mismatched-end 11-mer should not. Thus, RNAs of 11 and 12 nt should be indicative of incorrect (UTP) and correct (CTP) incorporation at position 11, respectively. Control experiments confirmed these expectations (Fig. 3.6B). UTP alone or a combination of UTP and CTP generated a 11-mer (lanes 5, 6, 17, and 18), but only the CTP-GTP combination (lanes 4 and 16), and not the UTP-GTP combination (lanes 3 and 15), led to efficient extension to 12 nt. The low concentration of GTP alone was not incorporated as a mismatch under these conditions (lanes 2 and 14). The small amount of 12-mer in lanes 3 and 15 is likely the result of UTP misincorporation at the matched end of the 11-mer. When all three NTPs are present, as expected, the amount of 12-mer (correct CTP incorporation) increases relative to the 11-mer (incorrect UTP incorporation) as the concentration of CTP was increased (Fig. 3.6B, lanes 7-12 and 19-24). The relative amounts of CTP and UTP utilization at position 11 were quantitated, and corrections were made for the small fraction of mismatched U that is extended by GTP (lanes 3 and 15), and for the appearance of the 13-mer that is likely derived from UTP misincorporation on the matched 3'-end of the 12-mer. The CTP/UTP utilization ratio, indicative of correct/incorrect incorporation, is nearly identical for pol II and pol IIΔ9 at each of the CTP concentrations used (Fig. 3.6C). These results are consistent with the more quantitative results in Fig. 3.5, where no evidence for decreased selectivity for pol IIΔ9 is observed.

Discussion

While the experiments described in this chapter were underway, Walmacq, C. *et al*. [20] published a paper describing a 5-fold decrease in the selectivity of pol II when Rpb9 is missing. I was not able to demonstrate a role for Rpb9 in selectivity in the A for C or U for C sequence context. The major differences between my results and those reported in that publication are in the misincorporation assays, where Walmacq, C. *et al.* [20] observed a much higher rate of UTP for CTP misincorporation (about 20-fold) and very large K_M for UTP (about 3 mM) that does not correlate well with my measured K_M for

ATP misincorporation or my obsevation that 1mM UTP is near saturation in a UTP-for-CTP misincorporation assay. One possible explanation for these differences is possible contamination of the UTP used by Walmacq, C. *et al*. [20] with low levels of CTP. In many lots of UTP from a number of suppliers, I have found only one lot from one company where the concentration of CTP was low enough that UTP misincorporation could be observed at all. While Walmacq, C. *et al*. [20] showed (based on electrophoretic mobility differences) that UTP misincorporation was observed at a UTP concentration of 100 µM, it is possible that at the much higher concentrations used in experiments in which they estimated K_M, sufficient CTP was present to interfere with misincorporation. This situation would lead to artificially high apparent K_M and V_{max} values for UTP misincorporation. Consistent with this explanation, the highest experimental concentration of UTP used by Walmacq, C. *et al*. [20] in their determination of K_M was 1.5 mM, where the rate versus [UTP] plot was nearly linear, and the hyperbolic fit to determine K_M and V_{max} was not very convincing. Misincorporation was verified in all of my experiments based on the slower kinetics of extension of a mismatched 3'-end compared to a matched 3'-end that would be generated by correct NTP contamination. In general, my observation is that almost all of the commercial pyrimidine NTPs are contaminated with low levels of other pyrimidines, and purine NTPs are contaminated with low levels of other purines. These levels are well within the purity limits set by most suppliers (99.9% pure). However, as shown in Fig 3.6, the rate of misincorporation of UTP at a concentration of 1 mM is about equal to the rate of correct CTP incorporation at a concentration of about 10 nM, which would be a contamination level of only 0.001%.

CHAPTER IV

FIDELITY OF RNA POLYMERASE II TRANSCRIPTION: ROLE OF RBP9 IN ERROR DETECTION AND PROOFREADING

Introduction

In addition to substrate selectivity, transcriptional fidelity can also depend on proofreading, in which mistakes can be excised from the growing transcript as it is synthesized. Pol II possesses an intrinsic nuclease activity that cleaves single nucleotides or short oligonucleotides from the 3'-ends of nascent RNAs, and this activity can be enhanced by the accessory protein TFIIS (reviewed in ref. [32]). Crystal structures of pol II-TFIIS complexes have revealed that a C-terminal zinc ribbon domain of TFIIS inserts into the active site of the polymerase where the side chains of two acidic residues (TFIIS D290 and E291 in *S. cerevisiae*) coordinate a metal and position a water molecule for hydrolysis [16, 48]. Deletion of *DST1*, the gene that encodes yeast TFIIS, has very little measureable effect in some *in vivo* assays designed to assess fidelity [40, 41], but easily detectable effects have been seen in others [42]. TFIIS, as well as its bacterial counterpart GreA, can stimulate removal of misincorporated NTPs *in vitro*, consistent with a possible role in proofreading [18, 44, 45].

Indirect evidence suggests that Rpb9 may also affect transcriptional proofreading. The Rpb9 homologs in RNA polymerases I and III (A12.2 and C11, respectively) are required for the intrinsic nuclease activity of these polymerases [29, 75, 90], which are much more robust than that of pol II, and the related archaeal protein TFS has been shown to affect transcriptional fidelity *in vitro* [30]. All of these proteins contain highly related N-terminal and C-terminal zinc ribbon domains characterized by the zinc chelating motif ($CX_2CX_nCX_2C$) [29, 30, 75, 76]. Moreover, a chimeric protein in which the C-terminal 35 amino acids of Rpb9 are replaced by the 25 C-terminal residues of C11 dramatically increases the intrinsic nuclease activity of pol II [78]. Other *in vitro*

experiments indicate that pol II lacking Rpb9 is less responsive to TFIIS-mediated transcript cleavage at defined pause and arrest sites [31, 44].

The work outlined in this study is the first direct examination of the potential roles of Rpb9 in transcriptional proofreading *in vitro*. I show that Rpb9 is important in slowing pol II elongation after a misincorporation event in order to provide a checkpoint during which proofreading can occur. I have identified two such checkpoints, one immediately after the incorrect NTP has been incorporated, and a second located one nucleotide downstream of the misincorporation. In addition, in at least some sequence contexts, Rpb9 is required for a pol II elongation complex (EC) containing an error at its 3'-end, or immediately adjacent to its 3'-end, to efficiently adopt a conformation in which TFIIS-mediated cleavage can occur.

Results

Absence of Rpb9 increases the rate of elongation beyond a mismatched 3'-end

Transcriptional proofreading involves competing rates of error propagation and error elimination. In order to explore the potential effect of Rbp9 on error propagation, purified pol II or pol IIΔ9 was immobilized with Ni^{2+}-NTA beads via a 6X-His tag on Rpb3, and ECs were assembled with DNA and RNA oligonucleotides [80] in which the 11 nt RNA was 5'-end labeled with ^{32}P (Fig. 3.1).

Using an EC with a G-U mismatch at its 3'-end to mimic a transcription error, we followed the time-course of extension with ATP (the next correct nucleotide) (Fig. 4.1B). The fraction extended to 12 nt was plotted against time and the data were fit to a single exponential equation (Fig. 4.1C). The rate of mismatch extension for pol IIΔ9 (k_{obs} = 1.1 min^{-1}) was 2-3 times faster than for pol II (k_{obs} = 0.44 min^{-1}). Assays with higher concentrations of ATP, up to 1 mM, gave essentially identical results, strongly suggesting that the ATP concentration used here (250 μM) is near saturating in this assay (data not shown). Interestingly, the number of complexes capable of being extended, which is generally 80-95% in assays in which the template and nascent RNA are completely complementary (data not shown), was significantly lower with these

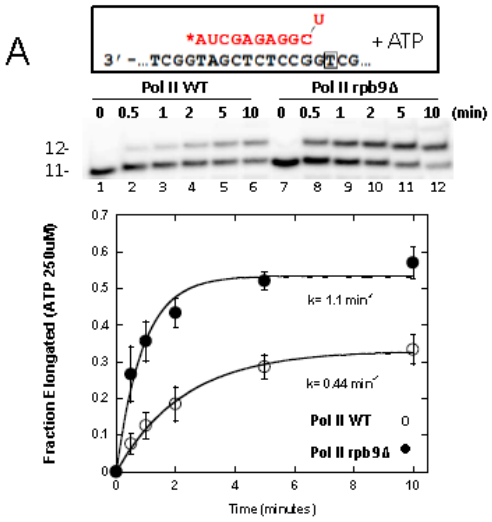

B

EC	Pol II	k_{obs} (min^{-1})
U / GA / CTGCT + GTP	WT	0.12 ± 0.01
	Rpb9Δ	0.34 ± 0.03
U / GA / CTGTC + ATP	WT	0.17 ± 0.02
	Rpb9Δ	0.53 ± 0.06
A / GA / CTGTC + ATP	WT	0.10 ± 0.01
	Rpb9Δ	0.28 ± 0.01

Fig. 4.1. Effect of Rpb9 on extension of a mismatched 3'-end. *A.* Schematic representation of the assembled elongation complex. Time course of 3'-mismatch extension. The EC depicted in A was assembled with purified pol II (lanes 1-6) or pol IIΔ9 (lanes 7-12) and incubated with ATP (250 μM). Aliquots were removed at the indicated times, and the products were fractionated by denaturing polyacrylamide gel electrophoresis and visualized on a phosphorimager. Quantitation of extension time course. The fraction of ECs extended to 12 nt was plotted versus time and fit to a single exponential equation (open circles, pol II; closed circles, pol IIΔ9). Error bars indicate the std. dev. for three independent experiments. B. Summary of 3'-mismatch extension rates for different sequence contexts. Rates of mismatch extension were determined with ECs that differed from that shown in A as depicted (with complementary template and non-template strands). The rate constants for extension with the next correct NTP (250 μM) were calculated for pol II and pol IIΔ9. Errors indicate the Chi Square value for the fit of the exponential curve to the averages of individual time points.

mismatched ECs; only about 30% of the pol II and 50% of the pol IIΔ9 complexes were extended at the reaction endpoints.

In order to explore mismatch extension in other sequence contexts, ECs were assembled in which the next correct NTP was changed from ATP to GTP, or in which either the penultimate or the mismatched ribonucleotide was altered. Each of the sequence changes had an effect on the absolute rate of mismatch extension, but in every context pol IIΔ9 was faster by 2-3 fold (Fig. 4.1D). Among the sequence contexts tested, the fastest rate observed was with an EC containing a G-C base pair just preceding a G-U mismatch. Extension rates determined by rapid quench kinetics using comparable ECs with completely matched RNAs have been reported to be 1000-fold or more higher than the rates we have determined with 3'-end-mismatched ECs [20]. Thus, a slow rate of mismatch extension provides a significant checkpoint that could be exploited for proofreading, as first described by Thomas, et al. [18]. The fraction of complexes that was subject to extension also varied in each of these sequence contexts, but, in contrast to the sequence context represented in Fig. 4.1A, the fraction of ECs that could be elongated in each of the other contexts was not significantly different for pol II and pol IIΔ9. This difference may depend on the G-C base pair immediately preceding the mismatch, as it is present only in the sequence context shown in Fig. 4.1A.

Rpb9 promotes TFIIS-mediated cleavage of transcripts with a mismatched 3'-end

The observed increase in the rate of error propagation in the absence of Rpb9 is relevant for fidelity only if it is not offset by a corresponding increase in the rate of error elimination. As has been observed in several studies [19, 31, 78], we have not detected significant endogenous cleavage activity with pol II ECs at near neutral pH. However, when ECs with mismatched 3'-ends were incubated in the presence of a cleavage-competent [91] N-terminal truncation of TFIIS (TFIISΔ2-146 [19]), relatively slow (k_{obs} = 0.05 min^{-1}) but efficient (65% cleavable) cleavage was apparent (Figs. 4.2A, lanes 1-8 and 2B, open circles). Furthermore, the observed removal of 2 nt from the RNA was as expected for a TFIIS-mediated process [37]. The cleaved RNAs remained in active ECs,

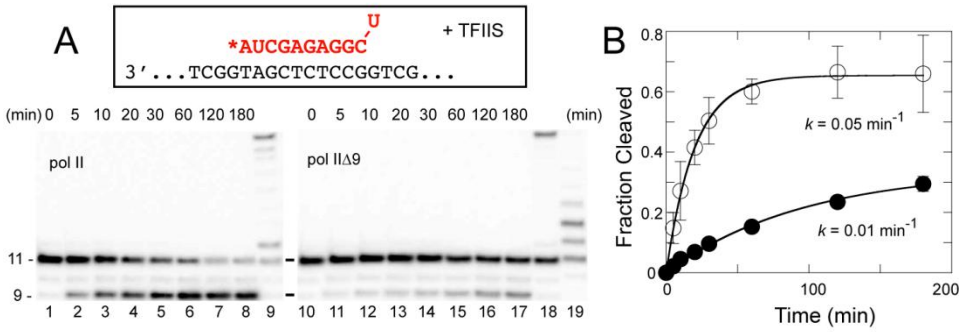

Fig. 4.2. Effect of Rpb9 on TFIIS-mediated cleavage of a 3'-mismatched end. *A*. Time course of cleavage. ECs with a mismatched 3'-end identical to that shown in Fig. 4.1A were assembled with purified pol II (lanes 1-9) or pol IIΔ9 (lanes 10-19). An abbreviated depiction of the EC is shown here for reference. These ECs were incubated with purified recombinant TFIIS (10 μM). Aliquots were removed at the indicated times, and the products were fractionated by denaturing polyacrylamide gel electrophoresis and visualized on a phosphorimager. After 180 min, ATP, CTP, and GTP (10 μM each) were added to the reaction and incubated for 30 sec (lanes 9 and 18). An aliquot of the pol IIΔ9 ECs was incubated for 60 min with ATP (250 μM) (lane 19). *B*. Quantitation of cleavage time course. The fraction of ECs cleaved to 9 nt was plotted against time and fit to a single exponential equation (open circles, pol II; closed circles, pol IIΔ9). Error bars indicate the std. dev. for three independent experiments.

as addition of ATP, CTP, and GTP (10 μM each) after 180 min resulted in rapid extension of the cleavage-generated 9-mer to longer products up to 20 nt, while the relatively small amount of 11-mer remaining (still containing the mismatch) was not efficiently extended during the 30 sec incubation with NTPs (Fig. 4.2A, compare lanes 8 and 9), as expected based on the slow rate of mismatch extension.

In an identical experiment with pol IIΔ9 ECs, cleavage was slower (k_{obs} = 0.01 min^{-1}) and less efficient (only about 30% cleavable) (Figs. 4.2A, lanes 10-17 and 4.2B, closed circles). As with the pol II ECs, all of the cleaved complexes remained in functional ECs that could be quickly elongated to 20 nt by addition of ATP, GTP, and CTP (10 μM each) (Fig. 4.2A, compare lanes 17 and 18). The different responses of pol II and pol IIΔ9 ECs was not the result of differential binding of TFIIS to the two types of complexes. The concentration of TFIIS used (10 μM) is sufficient to saturate both pol II and pol IIΔ9 ($K_d \approx 80$ nM for each [64]), and we confirmed that both the rate and the extent of cleavage were the same at TFIIS concentrations between 7 μM and 30 μM (data not shown).

These results demonstrate that Rpb9 affects transcriptional proofreading. The presence of Rpb9 slows extension of a mismatched 3'-end, and the impact of slower mismatch extension is not nullified by a corresponding decrease in the rate of TFIIS-mediated cleavage. In fact, for the sequence context used in Figs. 3.1B and 4.2, Rpb9 increases both the rate and efficiency of cleavage. In addition, our results are consistent with the idea that, at least in this sequence context, EC assembly with a mismatched 3'-end generates two classes of complexes that do not rapidly interconvert, one class that can be efficiently elongated (favored when Rpb9 is absent) and another that can be efficiently cleaved (favored when Rpb9 is present). This is most directly seen in Fig. 4.2A, lane 19, where complexes that are not cleavable can be elongated in the presence of the next correct NTP. The RNA products longer than 12 nt are likely the result of misincorporations or possible contamination of ATP with small amounts of GTP.

Interestingly, during preliminary experiments with 3'-end mismatched ECs in which pol II was immobilized from whole cell extracts (WCE), we noticed a significant amount

of RNA cleavage (generating a 9 nt RNA), during the assembly of the ECs, the extent of which correlated with the time taken for the preparation. To examine this in more detail, we prepared ECs as quickly as possible (Fig. 4.3A, lane 1) and then followed the time course of the cleavage reaction, which proceeded with a rate (k_{obs} = 0.048 min^{-1}) and extent (75% cleavable, including those that had been cleaved before time 0) similar to that seen with TFIIS in the purified system (Fig. 4.3A, lanes 2-6; Fig. 4.3B, open circles). As with the purified system, the cleaved RNAs remained in active ECs; addition of ATP, CTP, and GTP (10 µM each) after 60 min resulted in rapid extension of the cleavage-generated 9-mer to longer RNAs up to 20 nt, while the small amount of 11-mer remaining (still containing the mismatch) was not efficiently extended during a 30 sec incubation with NTPs (Fig. 4.3A, compare lanes 6 and 7). To determine whether this cleavage activity was TFIIS-dependent, we assembled ECs with pol II immobilized from WCE derived from an otherwise isogenic *dst1*Δ strain. These ECs carried out RNA extension as efficiently as those derived from WCE of *DST1* cells or assembled with purified pol II, but in the absence of *DST1*-encoded TFIIS, no cleavage activity was observed (data not shown). These results strongly suggest that the cleavage activity is mediated by TFIIS and that TFIIS stably and near stoichiometrically associates with pol II in the absence of an EC even after the extensive washes used in our immobilization protocol.

Pol II immobilized from a WCE prepared from an *rpb9*Δ strain also yielded results similar to those obtained with the purified system (Fig. 4.3A, lanes 8-13; Fig. 4.3B, closed circles). As observed in experiments with purified components, ECs containing a 3'-mismatch were less susceptible to cleavage than those with Rpb9 (approximately 40% cleavable, including those that had been cleaved before time 0), and all of the cleaved RNAs remained in functional ECs that could be quickly elongated to 20 nt by addition of ATP, GTP, and CTP (10 µM each) (Fig. 4.3A, compare lanes 13 and 14). As with the purified system, cleavage-resistant complexes were largely elongation-competent, which was demonstrated by their ability to incorporate ATP, the next correct nucleotide (Fig 4.3A, lane 15). (As in Fig. 4.2A, the RNAs larger than the expected 12 nt extension

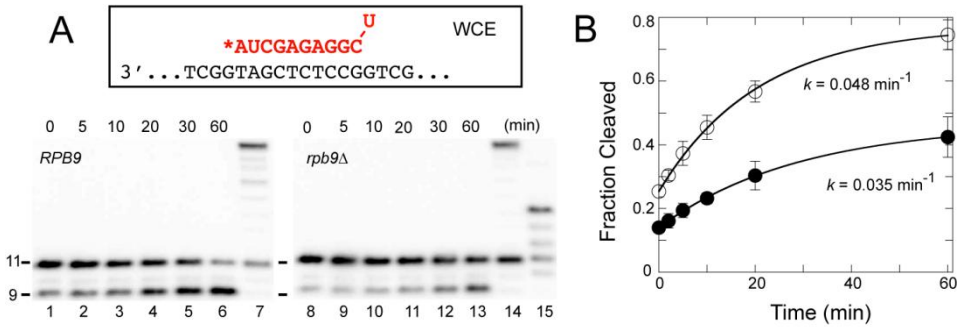

Fig. 4.3. Cleavage of mismatched 3'-ends by ECs assembled from WCE. *A*. Time course of cleavage. ECs with a mismatched 3'-end identical to that shown in Fig. 4.1A were assembled using WCE derived from *RPB9* (lanes 1-7) or *rpb9*Δ (lanes 8-15) yeast. An abbreviated depiction of the EC is shown here for reference. These ECs were incubated in TB(40). Aliquots were removed at the indicated times, and the products were fractionated by denaturing polyacrylamide gel electrophoresis and visualized on a phosphorimager. After 60 min, ATP, CTP, and GTP (10 µM each) were added to the reaction and incubated for 30 sec (lanes 7 and 14). An aliquot of the ECs assembled with WCE derived from *rpb9*Δ cells was incubated for 60 min with ATP (250 µM) (lane 15). *B*. Quantitation of cleavage time course. The fraction of ECs cleaved to 9 nt was plotted against time and fit to a single exponential equation (open circles, *RPB9* WCE; closed circles, *rpb9*Δ WCE). Error bars indicate the std. dev. for three independent experiments.

product were likely the result of misincorporation or small amounts of GTP contamination.) Approximately 40% of the WCE-derived pol IIΔ9 ECs had been cleaved at the reaction endpoint, suggesting that TFIIS is associated with at least 40% of these complexes. However, because this fraction is very similar to the fraction of cleavable complexes formed when purified TFIIS is present in excess (Fig. 4.2), and Rpb9 apparently has no effect on binding of TFIIS to pol II [64], TFIIS may actually be present in most, if not all, of the WCE-derived pol IIΔ9 ECs. One notable difference in our experiments with the purified and WCE systems is the faster rate of cleavage for pol IIΔ9 observed in the WCE system (k_{obs} = 0.035 min^{-1}). While this could be caused by unidentified WCE-derived proteins associated with the ECs, it might also be the result of native, intact TFIIS being present in the WCE system rather than the N-terminal truncated TFIIS used in the purified system. However, there are no experimental conditions in which it was observed that the increased rate of mismatch extension by pol IIΔ9 is countered by an increased rate or efficiency of TFIIS-mediated mismatch cleavage, and thus the absence of Rpb9 compromises the ability of pol II to proofread transcription errors.

It is possible that the effect of Rpb9 on the relative fractions of extendable and cleavable ECs containing a mismatched 3'-end could be an artifact of assembling the EC with a preformed mismatch. To test this idea, we generated a G-U mismatch *in situ* by misincorporating UTP (1 mM) into the matched 3'-end EC shown in Fig. 4.4A, using pol II (lanes 1-6) or pol IIΔ9 (lanes 7-12) immobilized from WCE. We verified that the 3'-ends of the extended complexes actually contained the mismatch by demonstrating that, unlike complexes with a matched end, they could not be rapidly extended by addition of NTPs (data not shown). This is not a trivial point, as some lots of NTPs are sufficiently contaminated that apparent misincorporation is actually caused by very low concentrations of contaminating correct nucleotide. The ECs were extensively washed to remove UTP and then followed over time to assess cleavage. Similar to the results with ECs assembled with the mismatched end (Figs. 4.2 and 4.3), the *in situ*-generated mismatch was much more efficiently cleaved when Rpb9 was present (Fig. 4.4A,

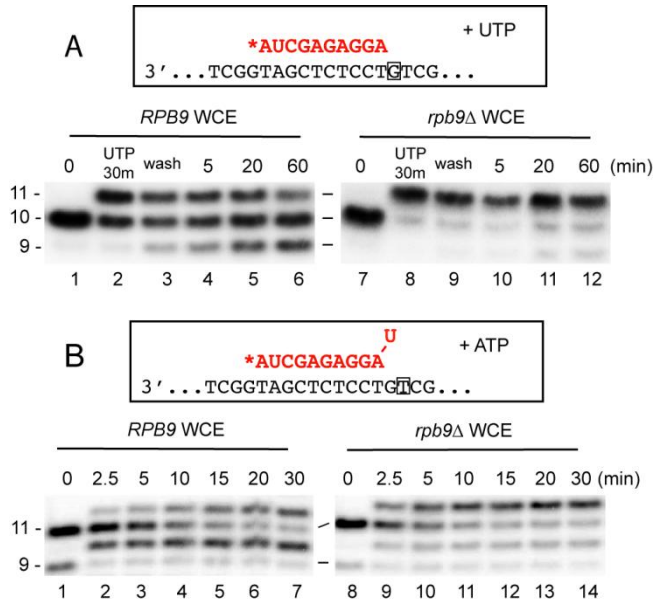

Fig. 4.4. Cleavage of in situ-generated 3'-end mismatches. *A*, ECs with a matched 3'-end were assembled using WCE derived from *RPB9* (lanes 1-6) or *rpb9*Δ (lanes 7-12) yeast. These ECs were identical to that shown in Fig. 4.1A except as depicted (and with complementary template and non-template strands). The ECs were incubated with UTP (1 mM) to generate a mismatched 3'-end (lanes 2 and 8), washed extensively to remove UTP (lanes 3 and 9), and then incubated in TB(40). Aliquots were removed at the indicated times (lanes 4-6 and 10-12), and the samples were fractionated by denaturing polyacrylamide gel electrophoresis and visualized on a phosphorimager. *B*. Effect of Rpb9 on proofreading a 3'-end mismatch. ECs with a mismatched 3'-end were assembled with WCE derived from *RPB9* (lanes 1-7) or *rpb9*Δ (lanes 8-14) yeast. These ECs were identical to that shown in Fig. 4.1A except as depicted (and with complementary template and non-template strands). The ECs were incubated with ATP (250 μM). Aliquots were removed at the indicated times, and the products were fractionated by denaturing polyacrylamide gel electrophoresis and visualized on a phosphorimager.

compare lanes 3-6 and 9-12). Note that the sequence context for the G-U mismatch is slightly different from that used in Fig. 4.2, suggesting that, although we have not checked a large variety of sequence contexts, the differential susceptibility to cleavage of pol II and pol IIΔ9 ECs is not limited to a specific context.

In a slightly different approach to assess the ability of Rpb9 to affect transcriptional proofreading, ECs were assembled with a mismatched 3'-end and then added ATP (the next correct nucleotide) (Fig. 4.4B), setting up conditions where both RNA extension and cleavage are possible. In this sequence context, cleavage of two nucleotides from the mismatched end generates a 9 nt product that can be rapidly extended by ATP, which is observed in the efficient extension of the 9 nt cleavage product generated during EC assembly (and present at time 0) to 10 nt during the first few minutes of the reaction (Fig. 4.4B, compare lanes 1 and 8 with lanes 2 and 9). Thus, in this experiment, direct extension of the 11 nt mismatched RNA generates a product of 12 nt, while cleavage of 2 nt generates a product of 10 nt after rapid extension of the resulting matched 9-mer by ATP. It is also possible that proofreading takes place after extension of the mismatch by cleavage of the extended 12-mer to 10 (see below). In either case, whether from cleavage of the mismatched 3'-end (11 nt) or the extended mismatched 3'-end (12 nt); the 10-mer represents a product derived from proofreading. Following the fate of the 11-mer present at time zero, over a period of 30 min approximately half was extended and half was cleaved using WCE containing pol II (Fig. 4.4B, lanes 1-7), while for WCE containing pol IIΔ9 only about 10% was cleaved, with most of the remainder extended to 12 nt (lanes 8-14). This experiment strongly supports the conclusion that proofreading is much more efficient in the presence of Rpb9.

Absence of Rpb9 increases the rate of elongation beyond a mismatched-matched 3'-end

If a transcription error is not removed before the mismatched end is extended, it is not clear at what point the mismatched base pair ceases to affect elongation or cleavage. In order to investigate this issue, we used purified pol II and pol IIΔ9 to assemble the EC shown in Fig. 4.5A, which is designed to have a mismatch followed by a matched 3'-end

to simulate a situation in which a transcription error at position 11 has not been removed prior to addition of the next NTP. GTP was added, and the time course of extension from 12 to 13 nt was monitored (Fig. 4.5). This experiment was performed at a low concentration of GTP to slow the reaction to a rate that could be easily measured. For pol II the rate of mismatch-match extension (k_{obs} = 0.29 min^{-1}) was approximately 1-2 orders of magnitude slower than would be expected under these conditions for a completely matched EC, based on a rate for the matched EC estimated from reported k_{pol} and K_M values [20]. Thus, this position provides a potential kinetic checkpoint subsequent to a transcription error that could be exploited in proofreading. The rate of mismatched-matched 3'-end extension for pol IIΔ9 (k_{obs} = 0.62 min^{-1}) was approximately two-fold faster than that for pol II, indicating a role for Rpb9 in establishing this checkpoint. The fraction of ECs that could be extended did not depend in any significant way on Rpb9; for both pol II and pol IIΔ9, about 70% of the ECs could be extended with GTP. (Note that the y-axis in Fig. 4.5B has been normalized to reflect only the ECs that are capable of being elongated.)

Rpb9 promotes TFIIS-mediated cleavage of a mismatched-matched 3'-end

To determine the potential for TFIIS-mediated proofreading of a mismatched-matched 3'-end, pol II and pol IIΔ9 immobilized from WCE were exploited. In the data presented earlier it was shown that TFIIS is stably associated with essentially all pol II and a minimum of 40% of pol IIΔ9. Similar to the results with a mismatched 3'-end (Fig. 4.3), some of the mismatch-matched ends were cleaved during the assembly of the ECs using WCE with pol II. Interestingly, a 10-mer was the only significant cleavage product (Fig. 4.6A, lane 1), indicating that the site of cleavage is between the mismatch and the nucleotide immediately preceding it. When GTP was added, ECs containing the mismatched-matched end were partitioned into two products, the cleaved 10-mer and a 13-mer resulting from extension with GTP (Fig. 4.6A, lanes 1-10). Both of these products were within functional elongation complexes, as they could be rapidly extended

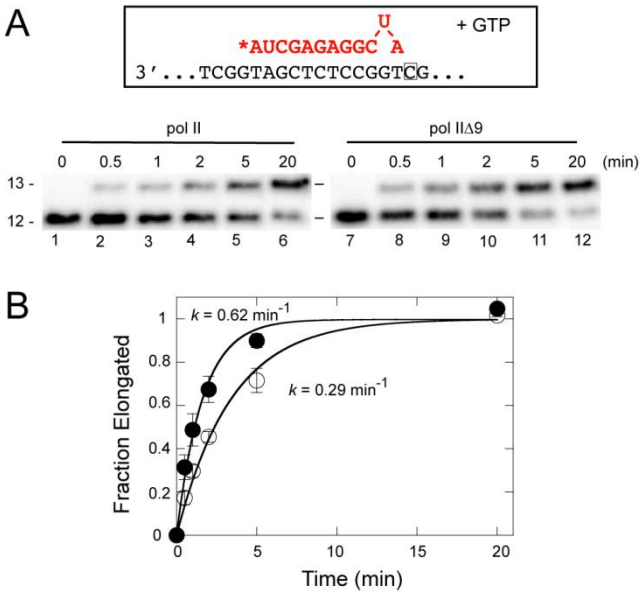

Fig. 4.5. Effect of Rpb9 on extension of a mismatch-matched 3'-end. *A*. Time course of extension. ECs with a mismatched-matched 3'-end were assembled with purified pol II (lanes 1-6) or pol IIΔ9 (lanes 7-12) and incubated with GTP (250 μM). These ECs were identical to that shown in Fig. 1A except as depicted (and with complementary template and non-template strands). Aliquots were removed at the indicated times, and the products were fractionated by denaturing polyacrylamide gel electrophoresis and visualized on a phosphorimager. *B*. Quantitation of extension time course. The fraction of ECs extended to 13 nt was plotted versus time and fit to a single exponential equation (open circles, pol II; closed circles, pol IIΔ9). Error bars indicate the std. dev. for three independent experiments. (Note that the y-axis has been normalized to reflect only the ECs that are capable being elongated.)

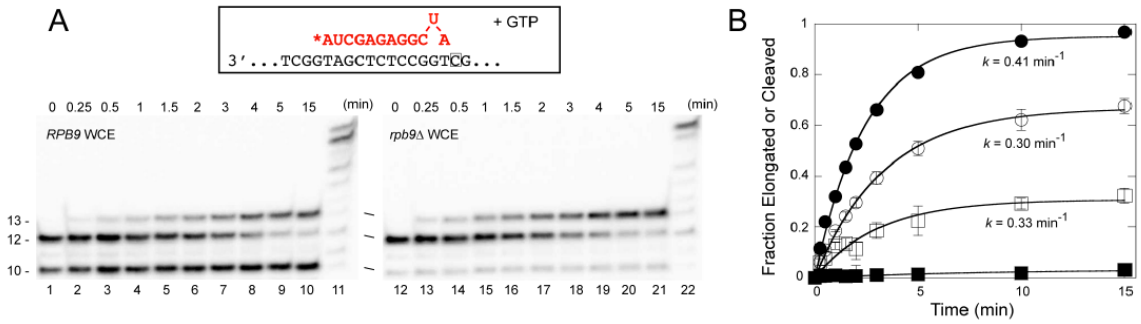

Fig. 4.6. Effect of Rpb9 on proofreading a mismatch-matched 3'-end. *A.* ECs with a mismatch-matched 3'-end were assembled with WCE derived from *RPB9* (lanes 1-11) or *rpb9*Δ (lanes 12-22) yeast. These ECs were identical to that shown in Fig. 4.1A except as depicted (and with complementary template and non-template strands). The ECs were incubated with GTP (1 μM). Aliquots were removed at the indicated times, and the products were fractionated by denaturing polyacrylamide gel electrophoresis and visualized on a phosphorimager. After 15 min, ATP and CTP (10 μM each) were added to the reaction and incubated for 30 sec (lanes 11 and 22). *B.* Quantitation of time course. The graph follows the extension or cleavage of ECs that contained a 12 nt RNA at time 0. ECs cleaved to 10 nt prior to time 0 are not included. Curves were derived from fits to a single exponential equation (open circles, *RPB9* WCE extension; open squares, *RPB9* WCE cleavage; closed circles, *rpb9*Δ WCE extension; closed squares, *rpb9*Δ WCE cleavage). Error bars indicate the std. deviation for three independent experiments.

by addition of ATP, GTP, and CTP (10 μM each) (Fig. 4.6A, lane 11). Taking into account only the 12-mer present at time zero, partitioning of the two products favored elongation by approximately 2-to-1, while the apparent rates of formation of the two products were essentially the same ($k_{obs} \approx 0.3$ min^{-1}) (Fig. 4.6B). (Note that the y-axis in Fig. 4.6B reflects only the fate of the 12-mer that is present at time zero.) These observations are consistent with two possible interpretations; either the rates of extension and cleavage are fortuitously identical, or there is a single population of pol II complexes containing the 12-mer that is subject to competing extension and cleavage reactions. In the latter case, partitioning of the two products would reflect the ratio of rate constants for the two reactions, while the identical observed rates would reflect their sum, giving estimates for the observed rate constants $k_{extension}$ and $k_{cleavage}$ to be approximately 0.2 min^{-1} and 0.1 min^{-1}, respectively.

ECs with the mismatched-matched end behaved quite differently with WCE-derived pol IIΔ9. Essentially no cleavage was observed, and the only product was the 13-mer generated by extension with GTP (Fig. 4.6A, lanes 12-21). In addition, the rate of extension (k_{obs} = 0.41 min^{-1}) (Fig. 4.6B) was about twice that estimated for pol II, consistent with the faster extension rate observed with the purified polymerases (Fig. 4.5). These results indicate that, in the absence of Rbp9, pol II is less able to take advantage of a potential proofreading checkpoint one nucleotide past a misincorporation event.

I also tested the ECs with a mismatch followed by two matched ribonucleotides at its 3'-end. Neither pol II nor pol IIΔ9 cleaved this RNA in the presence of TFIIS, and extension kinetics were indistinguishable from those expected for a completely matched RNA using the assays available (data not shown). Thus, it appears that misincorporation slows elongation and provides an opportunity for proofreading for only one nucleotide past the position at which the error was made.

Overall, these results strongly support a role for Rpb9 in transcriptional proofreading. In the absence of Rpb9, mismatched or mismatched-matched 3'-ends are 2- to 3-fold more rapidly extended, thus providing less time for removal of a

transcription error. This more rapid rate of extension is not offset by a more rapid rate of error removal, and, at least in some sequence contexts, the efficiency of cleavage is markedly decreased in the absence of Rbp9.

Discussion

In this study, the role of Rpb9 was addressed in aspects of fidelity related to proofreading. I have shown that pol IIΔ9 supports a faster rate of mismatch extension, decreasing the checkpoint period during which proofreading can occur, and that this faster extension is not offset by a faster rate of TFIIS-mediated error removal. In fact, error removal is slower in the absence of Rpb9, and, in at least some sequence contexts, the extent of cleavage is adversely affected as well, suggesting that Rpb9 can affect the efficiency with which ECs adopt a conformation favorable for TFIIS-mediated cleavage. Thus, Rpb9 can affect transcriptional proofreading in three ways, by decreasing the rate of error propagation, increasing the rate of TFIIS-mediated cleavage, and favoring formation of an EC conformation in which cleavage is possible.

These results can be interpreted in the context of X-ray crystal structures of ECs that contain RNAs with mismatched 3'-ends. Two types of structures have been observed. In one type [48], the polymerase is backtracked one nucleotide so that the last DNA-RNA base-pair is at position +1, and the mismatched 3'-end is in a novel location termed the P, or proofreading, site. This conformation is likely similar to the substrate for TFIIS-mediated cleavage between the -1 and +1 sites on the polymerase, resulting in the removal of 2 nt from the mismatched end of the RNA and generating a new, matched 3'-end ready for subsequent elongation. Our results are consistent with the idea that, at least in some sequence contexts, the presence of Rpb9 favors adoption of this backtracked, cleavage-competent conformation. In the second type of structure [42], the polymerase is essentially in the posttranslocated state, with the 3'-end mismatch at position -1 (present as a wobble base pair). Disruption and misalignment within the active site, including apparent loss of one of the catalytic metals, appears to preclude efficient extension of ECs in this conformation. Our results suggest that the absence of Rpb9 may favor a

similar conformation, which is not aligned to be cleavage-competent. In addition, if Rpb9 is important for establishing the active site disruptions, this posttranslocation positioning could explain the faster rate of mismatch extension observed in the absence of Rpb9, where the disruptions may not occur.

If a mismatch is not removed before extension to n*+1, further extension remains markedly slower than for an EC with RNA that is completely complementary to the template; this provides a second potential proofreading checkpoint. The mismatched-matched 3'-end in such ECs is subject to TFIIS-mediated cleavage, but further extension to n*+2 precludes cleavage. Pol IIΔ9 supports a faster rate of mismatch-match extension, limiting the opportunity for error removal at this checkpoint. Furthermore, pol IIΔ9 mismatched-matched ECs are almost exclusively in a conformation that allows extension but limits cleavage. Rpb9 can thus affect proofreading at this checkpoint by decreasing error propagation and enhancing error removal.

Sydow, *et al.* [21] have determined crystal structures of ECs containing mismatched-matched RNAs similar to those used in our study. In these structures the mismatch (a wobble T-U base pair) is at position -1, and the 3'-end, though complementary to the template, is in one of two "frayed" positions. This structure has been described as a "paused, frayed" EC representing the first step in the process of backtracking and cleavage [21]. Our results are consistent with the idea that mismatched-matched pol II complexes can backtrack one step from this conformation to allow TFIIS-mediated cleavage of 2 nt, while pol IIΔ9 complexes appear not to be able to efficiently backtrack and instead may favor the posttranslocated state, in which the next NTP can be added.

In summary, our results indicate that Rpb9 has multiple effects on transcriptional proofreading. After an error has been made, Rpb9 plays a role in slowing elongation to provide time for removal of the error, and it facilitates TFIIS-mediated RNA cleavage, at least in part by facilitating efficient rearrangement of the EC into a conformation

(presumably backtracked) necessary for cleavage. There appear to be at least two checkpoints at which Rpb9 can affect proofreading, either immediately after the error is introduced or after the error has been extended by addition of one nucleotide.

CHAPTER V

TRIGGER LOOP –DEPENDENT AND –INDEPENDENT FUNCTIONS OF THE RNA POLYMERASE II SUBUNIT RPB9

Introduction

Rpb9, a small subunit of RNA polymerase II, has emerged as an important element of transcription. Several lines of evidence indicate that Rpb9 is important for fidelity *in vivo* [40, 46]. Direct evidence presented in Chapter 3 identifies a role for Rpb9 in proofreading that is independent of TFIIS. In this chapter I examine the role of the pol II TL in Rpb9 function.

The TL is a critical structural feature of pol II's largest subunit Rpb1 and is required for cell viability in *S. cerevisae* [19]. The TL contains about 30 amino acids and it is proposed to have two essential conformations that reside in equilibrium. In the "open" conformation the TL is an unstructured loop positioned approximately 30 angstroms away from the active site [22]. In the "closed" conformation the TL forms an α-helical hairpin and swings toward the active center to make contact with the NTP in the insertion site [11]. The TL can be envisioned to work like a trap door over the active center to block the secondary channel entrance, providing functional groups that capture and position the correct nt for catalysis. Point mutations in the TL have varying effects that can result in an increase or decrease in the rate of transcription and selectivity [10, 57].

NTP addition can be considered as a two-step process. One way these steps can be observed is through the use of EDTA as the quenching agent in rapid quench-flow kinetic experiments. With the EDTA quench, a burst of activity, corresponding to rapid NTP binding, is observed, followed by a slower, reversible isomerization that sets up formation of the new phosphodiester bond [53]. This isomerization has been interpreted as the closing of the TL. The EDTA quench, by rapidly sequestering Mg^{2+}, prevents binding of NTP, but allows NTPs already in the active site to be added to the growing

RNA. It has been shown that pol IIΔ9 has a larger burst size than pol II, consistent with a longer dwell time in the active conformation in which the TL is closed, and thus allowing a larger fraction of bound NTP to be incorporated into RNA before it is released from the enzyme. This observation led to a model in which one role of Rpb9 is to assist in keeping the TL open, thereby slowing the rate of transcription [20].

The mushroom toxin α-amanitin is a specific and potent inhibitor of pol II transcription. It was first suggested from the crystal structure of pol II bound to α-amanitin [51], and based on kinetic studies [52], that the inhibitory effects on transcription arise from a blockage in translocation via the movable structural element referred to as the "bridge helix" (BH). Indeed, α-amanitin binds the funnel and pore just under the active site adjacent to the BH and TL; however, the single residue bound to α-amanitin was in a region of the BH that does not undergo movement [12]. Further refinement of the pol II/α-amanitin complex led to the discovery that α-amanitin directly interacts with the TL through one of its mobile residues, H1085. Transcription experiments *in vitro* substantiated the requirement of H1085 for α-amanitin inhibition utilizing H1085Y. H1085Y was shown to be resistant to α-amanitin in several assays measuring NTP incorporation rates and TFIIS mediated cleavage in "backtracked" ECs. It was reasoned from these findings that α-amanitin restricts TL movement solely through H1085, which is further supported by a lack of resistance in polymerases in which neighboring TL residues are mutated. Lastly, elongation rates measured in the presence of α-amanitin varied and were affected by the type of substrate used suggesting that α-amanitin may impede catalysis in addition to translocation, or at the very least the translocation effects are substrate-specific [19].

α-Amanitin provides an experimental tool to assess the role of the TL in Rpb9 function. If Rpb9 affects transcription solely through its proposed role in maintaining the TL in its open conformation, then in the presence of saturating concentrations of α-amanitin, where the TL is prevented from closing, the differences between pol II and pol IIΔ9 should disappear. In this chapter I describe the surprising observation that the effects of Rpb9 on addition of an incorrect, mismatched nt are completely dependent on

the TL, while its effects on addition of a correct, template-specified nt are independent of the TL, even if the 3'-end of the RNA contains a mismatch. These results suggest that the role of Rpb9 in proofreading checkpoint recognition (described in Chapter 4) does not require participation of the TL.

Results

Rbp9 effects on correct nucleotide extension of a matched 3'-end in the presence of α-amanitin

To determine the effect of α-amanitin on correct nt extension of an RNA with a 3'-end complementary to the template, pol II and pol IIΔ9 ECs, identical to those in Fig. 3.4C were assembled, and treated with α-amanitin (160 µg/mL). All four nucleoside triphosphates (1 mM) were then added, and the reactions were stopped at various times over a 1 hr period (Fig. 5.1A). This concentration of α-amanitin proved to be saturating for both pol II and pol IIΔ9 as concentrations as high as 640 µg/mL had no further effect on the rate of transcription (data not shown). The addition of α-amanitin severely inhibited the transcription rate (~50X) so the fraction of products that extended to 34 nt or greater was plotted against time, and the data were fit to a non-linear equation to determine the half time (Fig. 5.1B) under conditions where NTPs are saturating (see Fig. 3.4D). The actual number of nt synthesized (25) was divided by the half time to calculate the average rate of extension. As observed previously without α-amanitin, a two-fold difference in rate between pol II (*rate*= 0.05 ± 0.009 nt s^{-1}) and pol IIΔ9 (*rate*= 0.10 ± 0.016 nt s^{-1}) was maintained, which suggests a role for Rpb9 in "correct" nt elongation that is independent of the TL.

In addition, I performed a single nt addition assay to determine if the above two-fold effect persists when multiple translocation steps are not required and potential effects of pausing cannot contribute to the observed rate. To do this, I lowered the NTP concentration so that the rate was measurable by our methods. The EC complex pictured in Fig. 5.1C was assembled with both pol II and pol IIΔ9, followed by treatment with α-

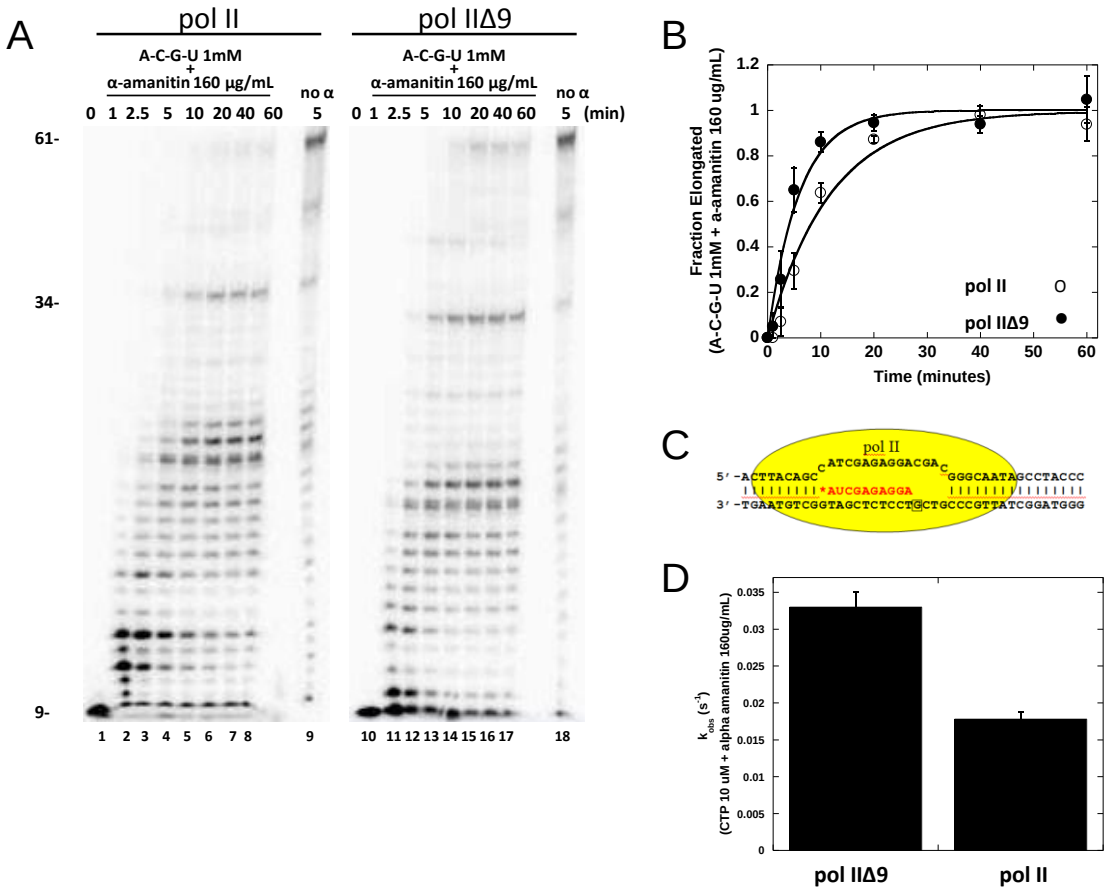

Fig. 5.1. Pol IIΔ9 increases the rate of elongation in the presence of α-amanitin. *A*, The rate of elongation was estimated by pre-incubating the EC shown in Fig. 3.4C, assembled using either pol II or pol IIΔ9, with α-amanitin for three minutes followed by simultaneous addition of ATP, CTP, GTP, and UTP. The concentration of each NTP added was 1000 µM. Each experiment was repeated three times to calculate standard deviation. The run-off product is indicated at 61 nt, however, RNAs 34 nt and greater were used for quantitation of the fraction elongated. *B*, The fraction elongated measured for pol II and pol IIΔ9 was plotted against time and the data were fit to a nonlinear equation to determine the halftime. To calculate the rate the actual number of nt synthesized (25) were divided by the half time. Open circle represents pol II and closed circle pol IIΔ9. *C*, EC used for single nt addition assay in the presence of α-amanitin. ECs were assembled with pol II or pol IIΔ9, treated with α-amanitin for three minutes and then followed by addition of CTP 10µM. Samples were collected over time and the fraction of RNAs extended with CTP was quantified. *D*, the graph shows the k_{obs} determined for pol II and pol IIΔ9. Each experiment was repeated three times to calculate standard deviation.

amanitin (160 µg/mL) and the template specified nt, CTP (10 µM). As consistent with the long-template assay, a two-fold difference in rate was measured even with the addition of one correct nt, pol II (k_{obs}= 0.017 s^{-1}) and pol IIΔ9 (k_{obs}= 0.033 s^{-1}) (Fig. 5.1D).

Rbp9 effects on misincorporation in the presence of α-amanitin

To assess the effect of α-amanitin on a misincorporation event, I assembled the EC pictured in Fig. 5.2A with both pol II and pol IIΔ9 and compared side by side, misincorporation, by adding ATP (1 mM) only (Fig. 5.2A lanes 2-7 and 15-20) and α-amanitin (160 µg/mL) plus ATP (1 mM) (Fig. 5.2A lanes 8-13 and 21-26). (Note that this is a slightly different sequence context than in Fig. 3.3C.). I also tested with up 640µg/mL α-amanitin to ensure that the ECs were saturated at this concentration. The extension of the completely matched 10nt RNA with ATP to 11nt was monitored over 1.5-2 hour time-period. The fraction of 11-mer derived from ECs either treated with α-amanitin (Fig. 5.2C) or untreated (Fig. 5.2B) were plotted against time and the data were fit to a single-exponential equation to determine k_{obs}. In the absence of α-amanitin, pol IIΔ9 (k_{obs} = 0.122 min^{-1}) is approximately two-times faster than pol II (k_{obs} = 0.069 min^{-1}). However, in the presence of α-amanitin the misincorporation rates for pol II and pol IIΔ9 are decreased 2 and 4 fold, respectively, and the two-fold difference in k_{obs} between pol II and pol IIΔ9 is no longer observed (0.029 min^{-1} vs. 0.025 min^{-1}). These results indicate that the effect of Rpb9 in this sequence context is completely dependent upon the TL. However, it is interesting to note that the misincorporation reaction in general is less dependent on the TL than correct extension, consistent with measurements made by Kaplan, C. D. *et al*. [19].

Rbp9 effects on mismatch extension in the presence of α-amanitin

One additional context in which Rpb9 has an effect on elongation is extension of a 3'-end mismatch, where Rpb9 slows elongation to provide time for proofreading (see Chapter 4). To assess the role of the TL in this process, ECs were assembled with pol II

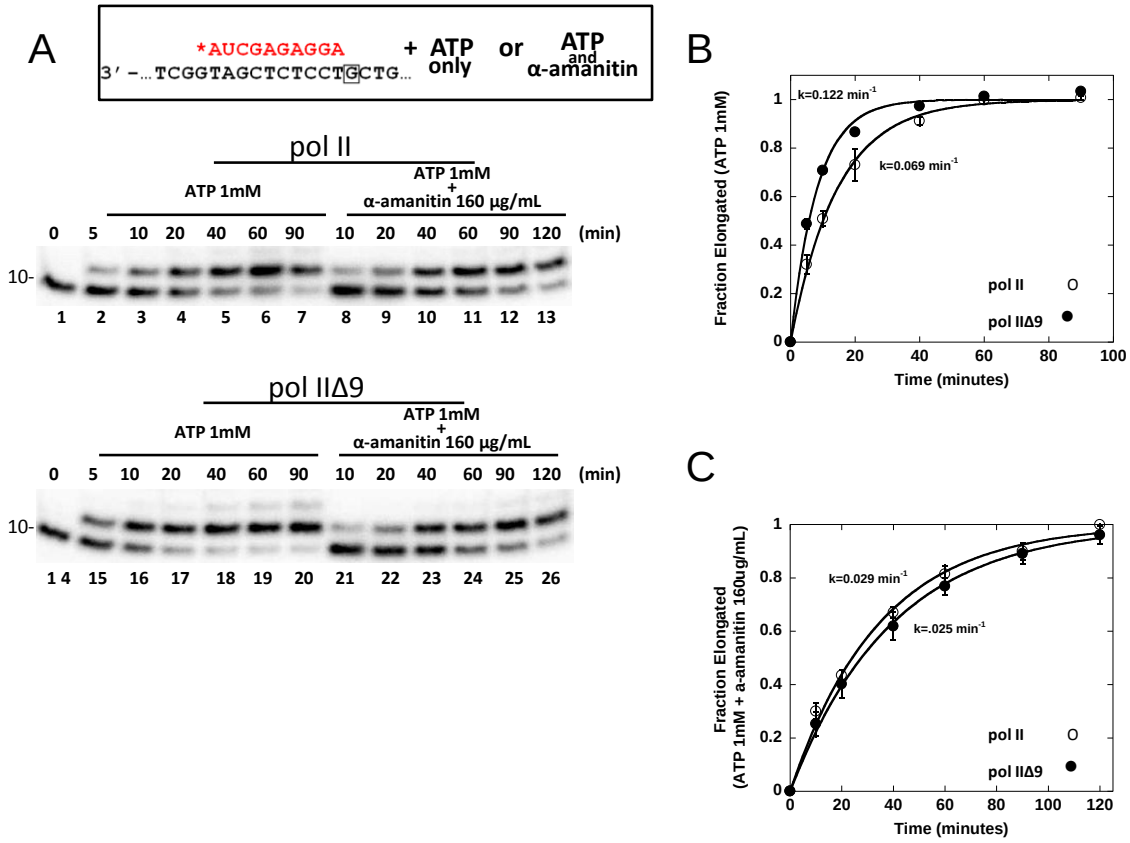

Fig. 5.2. Pol IIΔ9 increases the rate of ATP misincorporation only in the absence of α-amanitin. *A*, The box shows the abbreviated form of the EC in Fig. 4.2C. and the small box identifies the template nt that designates the nt at position (n), CTP. An incorrect nt, ATP 1mM, was added to the EC formed with pol II or pol IIΔ9 either with or without treatment with α-amanitin. The experiment was repeated three times at this concentration and gave almost identical rates at higher concentrations tested. *B*, The fraction of EC that extended with ATP to 11 nt or greater was plotted and fit to a single exponential equation to obtain k_{obs}. Open circle represents pol II and closed circle pol IIΔ9. To emphasize the difference in rate between pol II and pol IIΔ9 the fraction elongated was divided by the extent of the reaction, as determined from the fit. *C*, The fraction of EC that extended with ATP in the presence of α-amanitin to 11 nt or greater was plotted and fit to a single exponential equation to obtain k_{obs}. Open circle represents pol II and closed circle pol IIΔ9.The fraction elongated was divided by the extent of the reaction, as determined from the fit.

and pol IIΔ9 containing a RNA with a mismatched 3'-end (Fig. 5.3A). These ECs are identical to those used in the experiment in Fig. 4.1A. α-amanitin (160μg/mL) was added, and the time course of extension was determined in the presence of ATP (250 μM). This concentration is near saturation under these conditions, as an increase in concentration had no significant effect on the rate of extension (data not shown). In the presence of α-amanitin, mismatch extension is exceedingly slow, and time-points were collected over a 20 hour period. The fraction extended to 12nt or greater was plotted versus time, and the data were fit to a single exponential equation to obtain k_{obs} (Fig. 5.3B). The rates of extension (k_{obs} = $2.0x10^{-3}$ min^{-1} for pol II and k_{obs} = $4.0x10^{-3}$ min^{-1} for pol IIΔ9) are slower than the rates determined in the absence of α-amanitin (see Fig. 4.1) by over 200 fold. Interestingly, the 2-fold rate enhancement in pol IIΔ9 observed in the absence of α-amanitin (Fig. 4.1) is still apparent even in these exceedingly slow reactions, suggesting that Rpb9 affects mismatch-extension through a TL independent mechanism.

The slow reaction times raised the possibility that the ECs become non-functional during the extended reaction period. To determine if this could be a confounding aspect of this particular experiment, we tested the ECs for stability over time. To accomplish this, ATP (250μM) was added to ECs assembled at time zero, in the absence of α-amanitin, and then the reaction was stopped after 1 hour. An aliquot of the same ECs were allowed to stand for 20 hours at room temperature followed by addition of ATP (250μM) for 1 hour (compare Fig. 5.3A lanes 7 and 8, lanes 15 and 16). A significant amount of extension beyond the expected 12 nt reflects misincorporation events under these conditions. However, a high concentration and long incubation time was used purposely so that the number of potentially active ECs present could be assessed, and the consequence of this is misincorporation beyond 12 nt. The clear conclusion, however, is that the assembled ECs behave identically before and after the 20-hour incubation at room temperature.

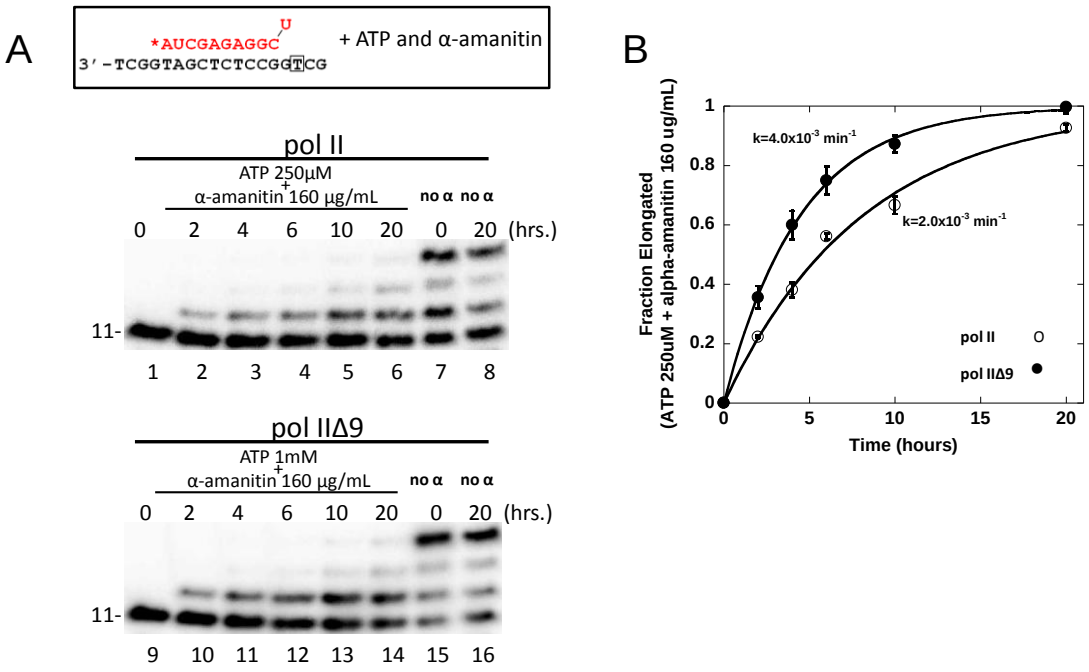

Fig. 5.3. Pol IIΔ9 increases the rate of mismatch extension in the presence of α-amanitin. *A*, The box shows the abbreviated form of the EC used and the small box identifies the template nt that designates the next correct nt at position (n+1), ATP. ECs were treated with α-amanitin (160 μg/mL) for three minutes prior to the addition of the next correct nt, ATP (250 μM). The reaction was stopped at various time-points. The experiment was repeated three times to calculate standard deviation. The zero and twenty hour time-points reflect addition of ATP to ECs prepared initially and to those incubated without NTP for a time period equivalent to the longest time-point taken, respectively. Both of these controls were obtained in the absence of α-amanitin and stopped after 1 hour exposure to ATP (250 μM). *B*, The fraction of ECs that were extended with ATP to 12 nt or greater in the presence of α-amanitin was plotted and fit to a single exponential equation to obtain k_{obs}. Open circle represents pol II and closed circle pol II Δ9.

Charged residues of Rpb9 (91-94) are dispensable both *in vivo* and *in vitro*

Rpb9 is located far from the active center of pol II (see Fig. 1.1). A mechanistic model explaining how Rpb9 might interact with the TL has been proposed [20]. In this model, the charged residues of the C-terminal domain of Rpb9 (^{91}RRKD^{94}) are proposed to be in close proximity to the open conformation of the TL and delay its closing (Fig. 5.4). In the absence of Rpb9, it was proposed that the TL resides more frequently in the closed conformation, which promotes catalysis and incorporation of an incorrect NTP. In the only published experimental test of this model, a K93A point mutation was constructed, but it had no effect on pol II behavior *in vitro*, and it was speculated that residues adjacent to K93 might be the ones important for the proposed interaction [20].

To more thoroughly test this model and determine if the flanking charged residues of K93 are important, we used site-directed PCR-mediated mutagenesis to construct plasmids (pRS416) bearing either a Rpb9 (91-94)A or Rpb9 K93E mutant. These mutants were tested *in vivo* by expressing them in *rpb9*Δ cells grown in the presence of several compounds to which *rpb9*Δ strains of yeast are hypersensitive, including cordycepin (3'-deoxyadenosine), a chain terminating nucleoside; menadione, an inducer of oxidative stress; and mycophenolic acid (MPA), an inhibitor of inosine monophosphate dehydrogenase that has been shown to reveal transcription start site defects at the *IMD2* gene (Fig. 5.5A). The *rpb9*Δ cells (*rpb9*Δ[vector]) exhibit a growth defect on synthetic-complete (SC) media compared to cells with an endogenous copy of *RPB9* (*RPB9*[vector]), or cells supplied with a plasmid-borne *RPB9* (*rpb9*Δ[*RPB9*]). The *rpb9*Δ cells expressing the *rpb9* mutants *(91-94)A* (*rpb9*Δ[*rpb9(91-94)A*]) and *K93E* (*rpb9*Δ[*rpb9 K93E*]) display growth identical to cells with a wt copy of *RPB9*. In fact, *(91-94)A* and *K93E* displayed wt growth under all conditions tested, with the exception of *K93E* grown on MPA, where a very slight growth defect can be observed.

Before evaluating these mutants *in vitro,* I verified that they would remain associated with pol II once the cells are lysed and exposed to the high salt washes associated with *in vitro* elongation complex assembly (see Chapter 2). All the plasmid-borne *RPB9* alleles were designed to have an N-terminal Flag-epitope to facilitate

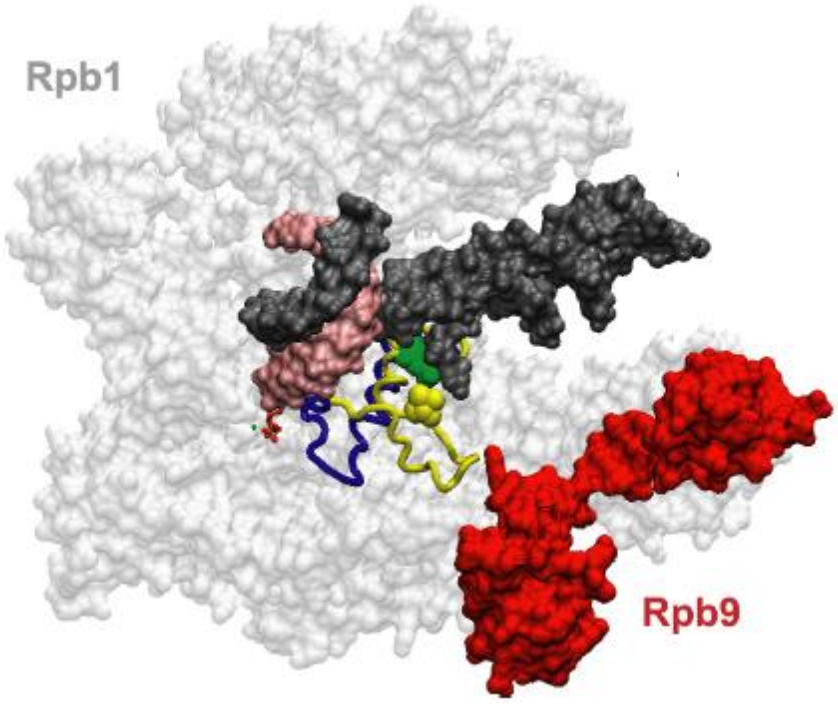

Fig. 5.4. Model for Rpb9 effect on selectivity. The structure is a pol II EC with an open TL in yellow and closed TL in blue. DNA is gray and RNA is pink. Residue E1103 is highlighted in orange and Rpb9 is shown in red. Modified from Walmaq, C *et al.*, *J. Biol. Chem*. 2009.

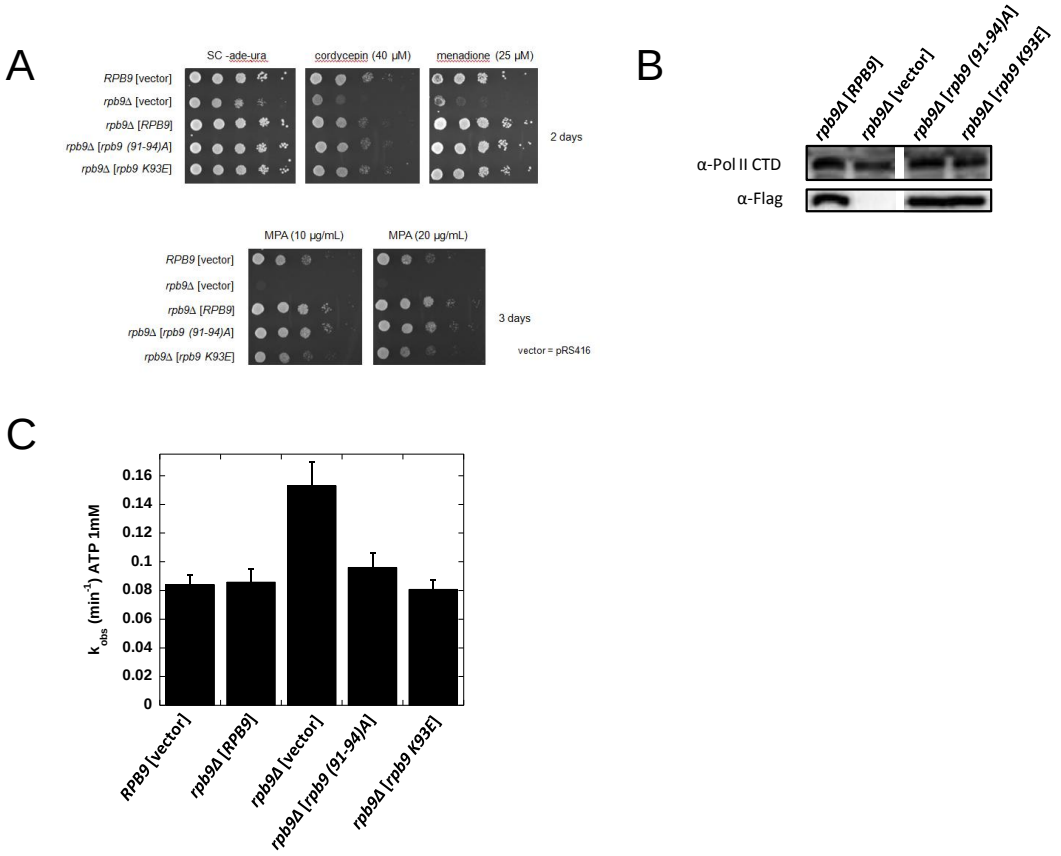

Fig. 5.5. Analysis of Rpb9 C-terminal loop residues. *A*, Spot tests reflect 10-fold serial dilutions of growth on minimal media or minimal media with the addition of drugs. Each strain has either an endogenous copy of *RPB9*, *Rpb9*, or C-terminal mutants of *Rpb9* expressed from a single-copy plasmid (pRS416). *B*, Western blot to show association of N-terminally Flag-tagged Rpb9 and mutants under the same conditions used for *in vitro* assays (see methods chapter). *C*, The graph shows k_{obs} measured for misincorporation of ATP, using WCEs to assembled ECs with the same sequence shown in Fig 4.4A. Each experiment was performed three times to calculate a standard deviation.

detection by immuno-blotting. In Fig. 5.5B pol II was immobilized from WCEs, exposing them to identical conditions used for *in vitro* assays. After denaturing SDS-PAGE and transfer to a nitrocellulose membrane they were probed with an α-Flag antibody. In each pol II immobilization, except pol II from *rpb9*Δ[vector] cells, a single band approximately 14 kDa was detected, which is consistent with the molecular weight of Rpb9 plus a Flag-tag sequence (lower box). Each sample was also probed with 8WG16, an antibody against the largest pol II subunit, Rpb1 (upper box). Quantitation of the bands indicated that the ratio of Rpb9 to Rpb1 derived from wt and mutant strains were essentially identical.

Next, the elongation effects of these mutants were tested *in vitro*. WCEs from all five strains shown in Fig. 5.5A were used to assemble ECs to test A for C misincorporation as done before. The k_{obs} was measured for the rate of extension with ATP (1mM) (Fig. 5.5C). As the *in vivo* data suggested, there is no effect of the Flag epitope on Rpb9 function, which is supported by similar rates of misincorporation for pol II from cells with an endogenous Rpb9 or plasmid-borne Flag-tagged Rpb9. In agreement with data using purified pol II, pol II from *rpb9*Δ cells is twice as fast at misincorporating ATP in this sequence context. Conversely, pol II from *rpb9(91-94)A* and *rpb9K93E* have rates similar to pol II from *RPB9*. \

Discussion

The proposed interaction of Rpb9 with the TL was evaluated by exploiting the inhibitory effects of α-amanitin. This drug has been shown to specifically target RNA pol II and restrict TL movement [19]. In my investigations, I have consistently observed, in all sequence contexts of NTP extension, a two-fold or more increase in elongation rate when pol II is lacking Rpb9. It would be expected that this difference in rate would disappear upon treatment with α-amanitin, if the increase in rate was due to an Rpb9 interaction with the TL. If the NTP extension does not involve the TL, it would be expected that the difference in rate would persist in the presence of α-amanitin. The overall results of these experiments is that Rpb9 appears to exert its effect on elongation

by at least two different mechanisms, TL-dependent and –independent, depending on whether the incoming NTP is the one specified by the DNA template.

I have shown that when pol II is missing Rpb9, the rate of correct nt extension from both a matched 3'-end and a mismatched 3'-end is at least two times faster than pol II with Rpb9 (Chapters 3 and 4). When these same ECs were treated with α-amanitin, the two-fold difference in rate remained, suggesting a TL-independent function for Rpb9 when the incoming NTP is complementary to the template. The TL has an obvious role in elongation, as the overall rate is markedly inhibited by α-amanitin, but the effect of Rpb9 is not dependent on the TL. One possibility is that Rpb9 limits the rate of extension with a base-paired NTP by influencing NTP alignment in the insertion site. As shown in Chapter 4, Rpb9 functions within the proofreading component of transcriptional fidelity by decreasing the rate of mismatch extension to allow for detection and removal of an error. The role of Rpb9 in allowing pol II to recognize an error does not appear to require the TL.

The results presented in this chapter also suggest a TL-dependent function for Rpb9 in the context of a misincorporation. In the presence of α-amanitin, the two-fold difference in misincorporation rate between pol II and pol IIΔ9 disappears. This indicates that Rpb9 and the TL function in the same pathway that leads to a misincorporation event. Interestingly, α-amanitin has comparatively little effect on the absolute rate of misincorporation, suggesting that misincorporation is much less dependent on the TL than extension with a template-matched NTP.

Specific residues of Rpb9 were proposed to be important for Rpb9-TL interaction by Walmacq, *et al*. [20]. In this model, the C-terminal charged loop (91-94) of Rpb9 directly interacts with the open form of the TL (Fig. 5.4), and in the absence of these residues, it was proposed that the TL would reside more frequently in the closed conformation, promoting catalysis with both correct and incorrect NTPs [20]. However, point mutations of some of these residues were shown to behave like wild-type pol II in the context of *in vivo* fidelity assays [46], *in vivo* start site selection and growth [56], and misincorporation *in vitro* [20].

I tested this model more completely by changing Rpb9 residues ^{91}RRKD^{94} to alanine. In all cases the *rpb9(91-94)A* grew or functioned catalytically like pol II. I further distorted this region by changing the charge of *K93*, which also behaved like wt in all assays tested. In previously published studies, these residues have been shown to be important for transcription in dC-tailed template readthrough assays, and for cleavage when pol II is arrested at pause sites [63], but I found no effect in cleavage assays using a mismatched 3'-end (data not shown). I also tested a *rpb9* mutation in which residues 88-97 were deleted, and this mutant behaved like pol IIΔ9 in A for C misincorporation assays. Consistent with these results, a *rpb9* Δ*89-95* mutant was shown to be sensitive to menadione *in vivo* [46] and cause readthrough defects *in vitro* [63]. Unfortunately, I was not able to demonstrate that this mutant was stably bound to pol II *in vitro*; however, all growth phenotypes tested for this mutant behaved like *RPB9*. It is possible that residues flanking amino acids 91-94 interact functionally with the TL, or modulate TL movement through other residues.

CHAPTER VI

SUMMARY

Fidelity of transcription ensures that RNA synthesized by pol II is an exact copy of the DNA template. Contributions to faithful transcription of a gene can occur before or just after phosphodiester bond formation between the RNA 3'-end and the NTP. Discrimination of the template specified NTP from the other NTPs and dNTPs describes the selectivity component of fidelity. Error propagation versus error removal defines the proofreading component of fidelity. When these systems malfunction, an error-prone pol II can introduce premature stop codons or other changes in the RNA transcript that can give rise to proteins that are potentially harmful to the cell. The small pol II subunit, Rpb9, was shown to be important for pol II transcription fidelity *in vivo [40]*. Transcription is a complicated process *in vivo* that involves an eclectic group of factors. However, the use of artificial elongation complexes *in vitro* can simplify and isolate particular aspects of transcription to help dissect and describe mechanisms of fidelity involving Rpb9.

When I started this project very little was known about Rpb9's role in pol II transcription fidelity. Yet, the structure of Rpb9 had been determined and Rpb9's affect on other aspects of transcription had been investigated. Rpb9 and Rpb4 are the only two subunits of pol II that are not required for cell viability in yeast. Deletion of the gene that encodes Rpb9 results in cells with several growth phenotypes and hypersensitivity to a variety of drugs [40, 45]. In addition, Rpb9 has two domains that each contain a zinc ribbon fold structure and are connected by a third linker domain [63]. Initial crystal structures of pol II revealed that contacts made between Rpb9 and pol II occur through its two largest subunits [7, 62]. The structure of Rpb9 is similar to subunits of pol I and pol II, and TFIIS, all of which have been reported to be important for maintaining transcriptional fidelity [29, 45, 63, 75, 76].

In early *in vitro* studies C-terminal mutants of Rpb9 were identified that resulted in decreased pause site recognition and prolonged duration of pausing at certain sites when

they were recognized. Rpb9 also enhanced TFIIS mediated cleavage of these pause sites [63]. Experiments conducted *in vivo* indicated that Rpb9 contributes to start site selection of some genes, and that only the N-terminal region of Rpb9 is necessary for wildtype start site selection and growth phenotypes [58, 59]. However, a direct role for Rpb9 in fidelity was not established until Nesser, N. K. *et al*. [40] demonstrated the loss of fidelity in yeast lacking the Rpb9 subunit [40].

Several *in vivo* and biochemical studies addressing pol II fidelity were published after I began this project. One of these reported a significant role for Rpb9 in selectivity, which was determined *in vitro* [20]. However, most of these studies focused on residues located in Rpb1's TL or BH that are important for fidelity. Crystal structures of pol II in ECs associated with the incorrect NTP, ECs with a mismatched 3'-end, or open and closed forms of the TL. These structures revealed possible fidelity intermediates that were then utilized to propose selectivity and proofreading mechanisms [12, 22], which were discussed in detail in Chapter I.

The role of Rpb9 in selectivity was explored in Chapter 3 utilizing several different methods. Selectivity was determined in two different ways by either determining catalytic efficiency, or estimating the selectivity ratio directly by providing conditions where the correct and incorrect NTP could compete. In both cases, and in all sequence contexts tested, Rpb9 had no significant effect on nt discrimination. These results conflict with a published study that reported a five-fold effect for Rpb9 on selectivity [20]. Possible reasons for these differences stem from the use of impure NTPs in that study and are discussed thoroughly in Chapter 3.

Rpb9 does, however, play a significant role in the proofreading capabilities of pol II, which was demonstrated in chapter 4. Rpb9 is critical for decreasing the rate of extension beyond an incorrect nt incorporation, but it also facilitates removal of an error. This type of mechanism for proofreading has been proposed for DNA pols [33] and pol III [28]. To facilitate this mechanism, Rpb9 may assist in the formation of complex that is cleavage competent and at the same time may disrupt an alignment of the RNA 3'-end that is conducive to catalysis. In the same way, Rpb9 can detect and aid in the removal

of an error that has been extended one nt. This suggests that Rpb9 is important for maintaining two different proofreading checkpoints, one that occurs immediately after mismatch formation and another that occurs one nt downstream of a misincorporated nt. The C-terminal residues of the BH (820-830) and the switch1/2 domains of Rpb1 shift position upon TFIIS binding. These movements can influence the alignment of the RNA 3'-end in the active site and may promote a cleavage competent conformation [15]. Rpb9 may facilitate the repositioning of these residues in the presence of TFIIS. The TL (1080-1105) also has a unique conformation when TFIIS binds pol II. The closed form of the TL occludes TFIIS access to the active site. In the absence of Rpb9 it was proposed that the TL equilibrium shifts from the open to the closed form [20], so it is also possible that Rpb9 promotes formation of a cleavage competent complex by modulating the movement of the TL. Mutants of these Rpb1 residues should be tested *in vivo*, and *in vitro* in the context of an *RPB9* delete and TFIIS.

In Chapter 5 I used α-amanitin as a means to determine TL-independent and TL-dependent functions of Rpb9 that are relevant to fidelity. Rpb9 was proposed to influence the equilibrium of TL movement from the open to the closed form, and this possibly occurs by direct interaction of Rpb9 with the TL [20]. The TL is critical for transcription elongation, and fidelity both *in vitro* and *in vivo*. Interestingly, deletion of the part of the Rpb1 gene that corresponds to the TL results in lethality in yeast. Not surprisingly, other Rpb1 mutants that affect TL movement also have an effect on fidelity [19, 53]. The potential interaction of Rpb9 with the TL was a promising route of exploration to gain more insight into Rpb9 fidelity mechanisms. In my investigations using α-amanitin, I found that Rpb9 slows the correct rate of nt extension of a RNA by a mechanism that is not completely dependent on the TL. This is also true in the case where the RNA 3'-end is mismatched with the DNA template, which provides some evidence that the TL is not absolutely required for Rpb9-mediated error recognition. In contrast, the effect of Rpb9 on incorporation of an incorrect nt is entirely dependent upon the TL. See the next section for a model consistent with these results.

Future directions

It would be interesting to further test residues flanking the Rpb9 C-terminal amino acids (91-94) and residues of Rpb1 that may interact with Rpb9 directly or indirectly utilizing growth and *in vitro* assays. A possible model for TL-independent and TL-dependent functions of Rpb9 is shown in Fig. 6.1, which is based on crystal structures and preliminary experiments done *in vivo* and *in vitro*. C-terminal residues (95-97) of Rpb9 are close to the loop of a Rpb1 helix-loop-helix structure. This loop, which I will refer to as the "anchor loop", is situated between Rpb1 alpha helices 20 and 21. Residue R711 of the anchor loop forms a hydrogen bond with Rpb9 residues S96 and has a hydrophobic stacking interaction with M97. I believe that Rpb9 remotely affects movement of the TL through interaction with the anchor loop, which may reflect the TL -dependent function of Rpb9. Anchor loop residues are much closer to the open form of the TL than any region of Rpb9. Direct interaction of the TL and Rpb9, which was proposed previously by Walmaq, C. *et al*. [20], is unlikely, and this is consistent with my experimental data shown in Chapter 5. In fact, anchor loop residue E712 can form a hydrogen bond with TL residue A1090, and M708 can form a hydrophobic stacking interaction with V1089. The TL-independent function of Rpb9 may involve positioning of helix 21, 22, or 23, which is also achieved via its interaction with the anchor loop. Another loop between helix 22 and 23, which I will refer to as the "K loop", extends a lysine (K752) into the active site that coordinates with the phosphate moiety of a correct NTP. Alteration of this lysine's position could affect catalysis. Work done by Kellinger, M. W. *et al*. [23] supports this idea. They demonstrated that positioning of the NTP in the active site can have a large effect on catalysis. In addition, a recent report showed the importance of helix 21, which houses a loss of function mutant Rpb1(G730D) [79]. To summarize, Rpb9 can directly interact with the anchor loop. This interaction may affect the equilibrium between the open and closed TL (TL-dependent), or the position of an active site lysine via helices of the K loop in the active site (TL-independent).

It would also be useful to study Rpb9's interaction with proteins other than those of pol II. Several genes have been identified as conferring a synthetic lethal phenotype

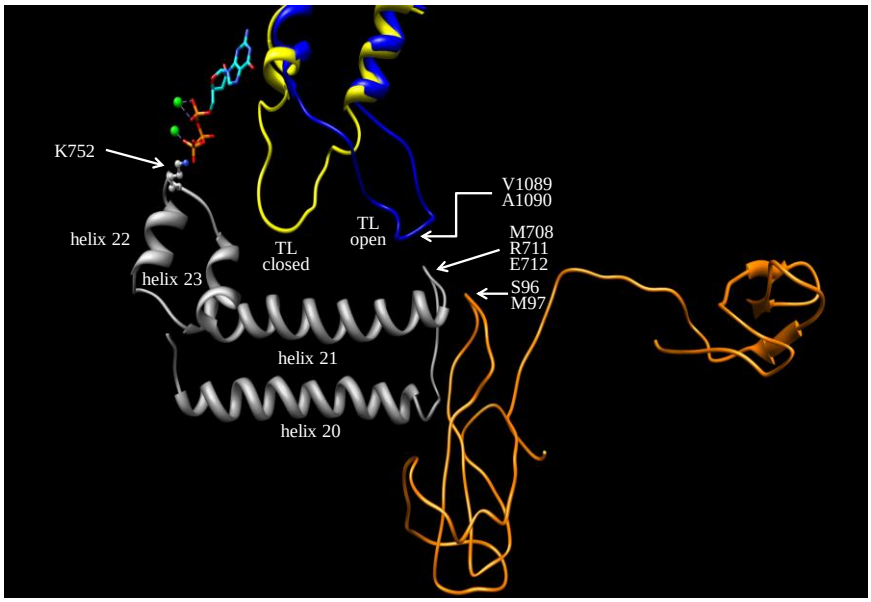

Fig. 6.1. Proposed model for TL-independent and TL-dependent functions of Rpb9. Rpb9 is shown in orange. Open TL is in blue and closed TL is yellow. Rpb1 helices 20-23 are gray. Magnesium A and B are represented by green spheres and indicate the position of the active site. NTP is shown in light blue and orange. Modified from an overlay of Protein Data Bank structures, ID code 2E2H and 1Y1W.

when deleted in the context of an *rpb9*Δ. The products of these genes are involved in a variety of processes that include transcription-coupled repair, chromatin modifications, initiation, elongation, and RNA processing. I have preliminary results that suggest Rpb9's role in maintenance of normal growth is derived from the N-terminal (Zn1) residues and elongation effects are delegated to the C-terminus (Zn2). If alleles of *RPB9* derived from random or targeted mutations yield proteins with different effects *in vivo* and *in vitro* they could be used to test for complementation of synthetic lethal phenotypes mentioned earlier to reveal regions of Rpb9 that are important in these processes.

REFERENCES

[1] A. Vannini, P. Cramer, Conservation between the RNA polymerase I, II, and III transcription initiation machineries, Mol Cell 45 (2012) 439-446.

[2] R.J. Sims, 3rd, R. Belotserkovskaya, D. Reinberg, Elongation by RNA polymerase II: the short and long of it, Genes Dev 18 (2004) 2437-2468.

[3] M. Palangat, D.R. Larson, Complexity of RNA polymerase II elongation dynamics, Biochim Biophys Acta 1819 (2012) 667-672.

[4] T.T. Saxowsky, P.W. Doetsch, RNA polymerase encounters with DNA damage: transcription-coupled repair or transcriptional mutagenesis?, Chem Rev 106 (2006) 474-488.

[5] F.J. Dennissen, N. Kholod, H.W. Steinbusch, F.W. Van Leeuwen, Misframed proteins and neurodegeneration: a novel view on Alzheimer's and Parkinson's diseases, Neurodegener Dis 7 (2010) 76-79.

[6] K. McKune, P.A. Moore, M.W. Hull, N.A. Woychik, Six human RNA polymerase subunits functionally substitute for their yeast counterparts, Mol Cell Biol 15 (1995) 6895-6900.

[7] P. Cramer, D.A. Bushnell, R.D. Kornberg, Structural basis of transcription: RNA polymerase II at 2.8 angstrom resolution, Science 292 (2001) 1863-1876.

[8] G. Orphanides, T. Lagrange, D. Reinberg, The general transcription factors of RNA polymerase II, Genes Dev 10 (1996) 2657-2683.

[9] L.A. Selth, S. Sigurdsson, J.Q. Svejstrup, Transcript Elongation by RNA Polymerase II, Annu Rev Biochem 79 (2010) 271-293.

[10] C.D. Kaplan, Basic mechanisms of RNA polymerase II activity and alteration of gene expression in Saccharomyces cerevisiae, Biochim Biophys Acta 1829 (2013) 39-54.

[11] E. Nudler, RNA polymerase active center: the molecular engine of transcription, Annu Rev Biochem 78 (2009) 335-361.

[12] F.W. Martinez-Rucobo, P. Cramer, Structural basis of transcription elongation, Biochim Biophys Acta 1829 (2013) 9-19.

[13] T.A. Steitz, A mechanism for all polymerases, Nature 391 (1998) 231-232.

[14] K.D. Westover, D.A. Bushnell, R.D. Kornberg, Structural basis of transcription: nucleotide selection by rotation in the RNA polymerase II active center, Cell 119 (2004) 481-489.

[15] H. Kettenberger, K.J. Armache, P. Cramer, Architecture of the RNA polymerase II-TFIIS complex and implications for mRNA cleavage, Cell 114 (2003) 347-357.

[16] H. Kettenberger, K.J. Armache, P. Cramer, Complete RNA polymerase II elongation complex structure and its interactions with NTP and TFIIS, Mol Cell 16 (2004) 955-965.

[17] K.A. Johnson, Conformational coupling in DNA polymerase fidelity, Annu Rev Biochem 62 (1993) 685-713.

[18] M.J. Thomas, A.A. Platas, D.K. Hawley, Transcriptional fidelity and proofreading by RNA polymerase II, Cell 93 (1998) 627-637.

[19] C.D. Kaplan, K.M. Larsson, R.D. Kornberg, The RNA polymerase II trigger loop functions in substrate selection and is directly targeted by alpha-amanitin, Mol Cell 30 (2008) 547-556.

[20] C. Walmacq, M.L. Kireeva, J. Irvin, Y. Nedialkov, L. Lubkowska, F. Malagon, J.N. Strathern, M. Kashlev, Rpb9 subunit controls transcription fidelity by delaying NTP sequestration in RNA polymerase II, J Biol Chem 284 (2009) 19601-19612.

[21] J.F. Sydow, F. Brueckner, A.C. Cheung, G.E. Damsma, S. Dengl, E. Lehmann, D. Vassylyev, P. Cramer, Structural basis of transcription: mismatch-specific fidelity mechanisms and paused RNA polymerase II with frayed RNA, Mol Cell 34 (2009) 710-721.

[22] X. Liu, D.A. Bushnell, R.D. Kornberg, RNA polymerase II transcription: structure and mechanism, Biochim Biophys Acta 1829 (2013) 2-8.

[23] M.W. Kellinger, S. Ulrich, J. Chong, E.T. Kool, D. Wang, Dissecting chemical interactions governing RNA polymerase II transcriptional fidelity, J Am Chem Soc 134 (2012) 8231-8240.

[24] E. Kashkina, M. Anikin, F. Brueckner, R.T. Pomerantz, W.T. McAllister, P. Cramer, D. Temiakov, Template misalignment in multisubunit RNA polymerases and transcription fidelity, Mol Cell 24 (2006) 257-266.

[25] C.M. Joyce, S.J. Benkovic, DNA polymerase fidelity: kinetics, structure, and checkpoints, Biochemistry 43 (2004) 14317-14324.

[26] D.A. Erie, O. Hajiseyedjavadi, M.C. Young, P.H. von Hippel, Multiple RNA polymerase conformations and GreA: control of the fidelity of transcription, Science 262 (1993) 867-873.

[27] N. Zenkin, Y. Yuzenkova, K. Severinov, Transcript-assisted transcriptional proofreading, Science 313 (2006) 518-520.

[28] N. Alic, N. Ayoub, E. Landrieux, E. Favry, P. Baudouin-Cornu, M. Riva, C. Carles, Selectivity and proofreading both contribute significantly to the fidelity of RNA polymerase III transcription, Proc Natl Acad Sci U S A 104 (2007) 10400-10405.

[29] C.D. Kuhn, S.R. Geiger, S. Baumli, M. Gartmann, J. Gerber, S. Jennebach, T. Mielke, H. Tschochner, R. Beckmann, P. Cramer, Functional architecture of RNA polymerase I, Cell 131 (2007) 1260-1272.

[30] U. Lange, W. Hausner, Transcriptional fidelity and proofreading in Archaea and implications for the mechanism of TFS-induced RNA cleavage, Mol Microbiol 52 (2004) 1133-1143.

[31] R.G. Weilbaecher, D.E. Awrey, A.M. Edwards, C.M. Kane, Intrinsic transcript cleavage in yeast RNA polymerase II elongation complexes, J Biol Chem 278 (2003) 24189-24199.

[32] R.N. Fish, C.M. Kane, Promoting elongation with transcript cleavage stimulatory factors, Biochim Biophys Acta 1577 (2002) 287-307.

[33] J.P. Gill, J. Wang, D.P. Millar, DNA polymerase activity at the single-molecule level, Biochem Soc Trans 39 (2011) 595-599.

[34] Y. Yuzenkova, A. Bochkareva, V.R. Tadigotla, M. Roghanian, S. Zorov, K. Severinov, N. Zenkin, Stepwise mechanism for transcription fidelity, BMC Biol 8 (2010) 54.

[35] F.W. van Leeuwen, D.F. Fischer, D. Kamel, J.A. Sluijs, M.A. Sonnemans, R. Benne, D.F. Swaab, A. Salehi, E.M. Hol, Molecular misreading: a new type of transcript mutation expressed during aging, Neurobiol Aging 21 (2000) 879-891.

[36] F.W. van Leeuwen, P. van Tijn, M.A. Sonnemans, B. Hobo, D.M. Mann, C. Van Broeckhoven, S. Kumar-Singh, P. Cras, G. Leuba, A. Savioz, M.L. Maat-Schieman, H. Yamaguchi, J.M. Kros, W. Kamphorst, E.M. Hol, R.A. de Vos,

D.F. Fischer, Frameshift proteins in autosomal dominant forms of Alzheimer disease and other tauopathies, Neurology 66 (2006) S86-92.

[37] M.G. Izban, D.S. Luse, SII-facilitated transcript cleavage in RNA polymerase II complexes stalled early after initiation occurs in primarily dinucleotide increments, J Biol Chem 268 (1993) 12864-12873.

[38] V.K. Olmsted, D.E. Awrey, C. Koth, X. Shan, P.E. Morin, S. Kazanis, A.M. Edwards, C.H. Arrowsmith, Yeast transcript elongation factor (TFIIS), structure and function. I: NMR structural analysis of the minimal transcriptionally active region, J Biol Chem 273 (1998) 22589-22594.

[39] K. Agarwal, K.H. Baek, C.J. Jeon, K. Miyamoto, A. Ueno, H.S. Yoon, Stimulation of transcript elongation requires both the zinc finger and RNA polymerase II binding domains of human TFIIS, Biochemistry 30 (1991) 7842-7851.

[40] N.K. Nesser, D.O. Peterson, D.K. Hawley, RNA polymerase II subunit Rpb9 is important for transcriptional fidelity in vivo, Proc Natl Acad Sci U S A 103 (2006) 3268-3273.

[41] R.J. Shaw, N.D. Bonawitz, D. Reines, Use of an in vivo reporter assay to test for transcriptional and translational fidelity in yeast, J Biol Chem 277 (2002) 24420-24426.

[42] H. Koyama, T. Ito, T. Nakanishi, N. Kawamura, K. Sekimizu, Transcription elongation factor S-II maintains transcriptional fidelity and confers oxidative stress resistance, Genes Cells 8 (2003) 779-788.

[43] S. Sigurdsson, A.B. Dirac-Svejstrup, J.Q. Svejstrup, Evidence that transcript cleavage is essential for RNA polymerase II transcription and cell viability, Mol Cell 38 (2010) 202-210.

[44] D.A. Erie, T.D. Yager, P.H. von Hippel, The single-nucleotide addition cycle in transcription: a biophysical and biochemical perspective, Annu Rev Biophys Biomol Struct 21 (1992) 379-415.

[45] C. Jeon, K. Agarwal, Fidelity of RNA polymerase II transcription controlled by elongation factor TFIIS, Proc Natl Acad Sci U S A 93 (1996) 13677-13682.

[46] H. Koyama, T. Ito, T. Nakanishi, K. Sekimizu, Stimulation of RNA polymerase II transcript cleavage activity contributes to maintain transcriptional fidelity in yeast, Genes Cells 12 (2007) 547-559.

[47] A.C. Cheung, P. Cramer, Structural basis of RNA polymerase II backtracking, arrest and reactivation, Nature 471 (2011) 249-253.

[48] D. Wang, D.A. Bushnell, X. Huang, K.D. Westover, M. Levitt, R.D. Kornberg, Structural basis of transcription: backtracked RNA polymerase II at 3.4 angstrom resolution, Science 324 (2009) 1203-1206.

[49] D. Wang, D.A. Bushnell, K.D. Westover, C.D. Kaplan, R.D. Kornberg, Structural basis of transcription: role of the trigger loop in substrate specificity and catalysis, Cell 127 (2006) 941-954.

[50] F. Brueckner, P. Cramer, Structural basis of transcription inhibition by alpha-amanitin and implications for RNA polymerase II translocation, Nat Struct Mol Biol 15 (2008) 811-818.

[51] D.A. Bushnell, P. Cramer, R.D. Kornberg, Structural basis of transcription: alpha-amanitin-RNA polymerase II cocrystal at 2.8 A resolution, Proc Natl Acad Sci U S A 99 (2002) 1218-1222.

[52] X.Q. Gong, Y.A. Nedialkov, Z.F. Burton, Alpha-amanitin blocks translocation by human RNA polymerase II, J Biol Chem 279 (2004) 27422-27427.

[53] M.L. Kireeva, Y.A. Nedialkov, G.H. Cremona, Y.A. Purtov, L. Lubkowska, F. Malagon, Z.F. Burton, J.N. Strathern, M. Kashlev, Transient reversal of RNA polymerase II active site closing controls fidelity of transcription elongation, Mol Cell 30 (2008) 557-566.

[54] M.H. Larson, J. Zhou, C.D. Kaplan, M. Palangat, R.D. Kornberg, R. Landick, S.M. Block, Trigger loop dynamics mediate the balance between the transcriptional fidelity and speed of RNA polymerase II, Proc Natl Acad Sci U S A 109 (1991) 6555-6560.

[55] N.A. Woychik, W.S. Lane, R.A. Young, Yeast RNA polymerase II subunit RPB9 is essential for growth at temperature extremes, J Biol Chem 266 (1991) 19053-19055.

[56] S.A. Hemming, D.B. Jansma, P.F. Macgregor, A. Goryachev, J.D. Friesen, A.M. Edwards, RNA polymerase II subunit Rpb9 regulates transcription elongation in vivo, J Biol Chem 275 (2000) 35506-35511.

[57] C.D. Kaplan, H. Jin, I.L. Zhang, A. Belyanin, Dissection of Pol II trigger loop function and Pol II activity-dependent control of start site selection in vivo, PLoS Genet 8 (2012) e1002627.

[58] Z.W. Sun, A. Tessmer, M. Hampsey, Functional interaction between TFIIB and the Rpb9 (Ssu73) subunit of RNA polymerase II in Saccharomyces cerevisiae, Nucleic Acids Res 24 (1996) 2560-2566.

[59] M.W. Hull, K. McKune, N.A. Woychik, RNA polymerase II subunit RPB9 is required for accurate start site selection, Genes Dev 9 (1995) 481-490.

[60] S. Li, M.J. Smerdon, Rpb4 and Rpb9 mediate subpathways of transcription-coupled DNA repair in Saccharomyces cerevisiae, EMBO J 21 (2002) 5921-5929.

[61] S. Li, B. Ding, R. Chen, C. Ruggiero, X. Chen, Evidence that the transcription elongation function of Rpb9 is involved in transcription-coupled DNA repair in Saccharomyces cerevisiae, Mol Cell Biol 26 (2006) 9430-9441.

[62] A.L. Gnatt, P. Cramer, J. Fu, D.A. Bushnell, R.D. Kornberg, Structural basis of transcription: an RNA polymerase II elongation complex at 3.3 A resolution, Science 292 (2001) 1876-1882.

[63] S.A. Hemming, A.M. Edwards, Yeast RNA polymerase II subunit RPB9. Mapping of domains required for transcription elongation, J Biol Chem 275 (2000) 2288-2294.

[64] D.E. Awrey, R.G. Weilbaecher, S.A. Hemming, S.M. Orlicky, C.M. Kane, A.M. Edwards, Transcription elongation through DNA arrest sites. A multistep process involving both RNA polymerase II subunit RPB9 and TFIIS, J Biol Chem 272 (1997) 14747-14754.

[65] V. Van Mullem, M. Wery, M. Werner, J. Vandenhaute, P. Thuriaux, The Rpb9 subunit of RNA polymerase II binds transcription factor TFIIE and interferes with the SAGA and elongator histone acetyltransferases, J Biol Chem 277 (2002) 10220-10225.

[66] E. Milgrom, R.W. West, Jr., C. Gao, W.C. Shen, TFIID and Spt-Ada-Gcn5-acetyltransferase functions probed by genome-wide synthetic genetic array analysis using a Saccharomyces cerevisiae taf9-ts allele, Genetics 171 (2005) 959-973.

[67] M. Wery, E. Shematorova, B. Van Driessche, J. Vandenhaute, P. Thuriaux, V. Van Mullem, Members of the SAGA and Mediator complexes are partners of the transcription elongation factor TFIIS, EMBO J 23 (2004) 4232-4242.

[68] T. Xiao, C.F. Kao, N.J. Krogan, Z.W. Sun, J.F. Greenblatt, M.A. Osley, B.D. Strahl, Histone H2B ubiquitylation is associated with elongating RNA polymerase II, Mol Cell Biol 25 (2005) 637-651.

[69] F. Malagon, A.H. Tong, B.K. Shafer, J.N. Strathern, Genetic interactions of DST1 in Saccharomyces cerevisiae suggest a role of TFIIS in the initiation-elongation transition, Genetics 166 (2004) 1215-1227.

[70] C. Gonzalez-Aguilera, C. Tous, R. Babiano, J. de la Cruz, R. Luna, A. Aguilera, Nab2 functions in the metabolism of RNA driven by polymerases II and III, Mol Biol Cell 22 (2011) 2729-2740.

[71] H. Gaillard, C. Tous, J. Botet, C. Gonzalez-Aguilera, M.J. Quintero, L. Viladevall, M.L. Garcia-Rubio, A. Rodriguez-Gil, A. Marin, J. Arino, J.L. Revuelta, S. Chavez, A. Aguilera, Genome-wide analysis of factors affecting transcription elongation and DNA repair: a new role for PAF and Ccr4-not in transcription-coupled repair, PLoS Genet 5 (2009) e1000364.

[72] S. Holbein, A. Wengi, L. Decourty, F.M. Freimoser, A. Jacquier, B. Dichtl, Cordycepin interferes with 3' end formation in yeast independently of its potential to terminate RNA chain elongation, RNA 15 (2009) 837-849.

[73] P.A. Gibney, T. Fries, S.M. Bailer, K.A. Morano, Rtr1 is the Saccharomyces cerevisiae homolog of a novel family of RNA polymerase II-binding proteins, Eukaryot Cell 7 (2008) 938-948.

[74] X. Chen, C. Ruggiero, S. Li, Yeast Rpb9 plays an important role in ubiquitylation and degradation of Rpb1 in response to UV-induced DNA damage, Mol Cell Biol 27 (2007) 4617-4625.

[75] S. Chedin, M. Riva, P. Schultz, A. Sentenac, C. Carles, The RNA cleavage activity of RNA polymerase III is mediated by an essential TFIIS-like subunit and is important for transcription termination, Genes Dev 12 (1998) 3857-3871.

[76] S.K. Whitehall, C. Bardeleben, G.A. Kassavetis, Hydrolytic cleavage of nascent RNA in RNA polymerase III ternary transcription complexes, J Biol Chem 269 (1994) 2299-2306.

[77] B.P. Kaine, I.J. Mehr, C.R. Woese, The sequence, and its evolutionary implications, of a Thermococcus celer protein associated with transcription, Proc Natl Acad Sci U S A 91 (1994) 3854-3856.

[78] W. Ruan, E. Lehmann, M. Thomm, D. Kostrewa, P. Cramer, Evolution of two modes of intrinsic RNA polymerase transcript cleavage, J Biol Chem 286 (2011) 18701-18707.

[79] H. Koyama, T. Ueda, T. Ito, K. Sekimizu, Novel RNA polymerase II mutation suppresses transcriptional fidelity and oxidative stress sensitivity in rpb9Delta yeast, Genes Cells 15 (2010) 151-159.

[80] M.L. Kireeva, L. Lubkowska, N. Komissarova, M. Kashlev, Assays and affinity purification of biotinylated and nonbiotinylated forms of double-tagged core RNA polymerase II from Saccharomyces cerevisiae, Methods Enzymol 370 (2003) 138-155.

[81] A. Baudin, O. Ozier-Kalogeropoulos, A. Denouel, F. Lacroute, C. Cullin, A simple and efficient method for direct gene deletion in Saccharomyces cerevisiae, Nucleic Acids Res 21 (1993) 3329-3330.

[82] C.B. Brachmann, A. Davies, G.J. Cost, E. Caputo, J. Li, P. Hieter, J.D. Boeke, Designer deletion strains derived from Saccharomyces cerevisiae S288C: a useful set of strains and plasmids for PCR-mediated gene disruption and other applications, Yeast 14 (1998) 115-132.

[83] L. de Mercoyrol, Y. Corda, C. Job, D. Job, Accuracy of wheat-germ RNA polymerase II. General enzymatic properties and effect of template conformational transition from right-handed B-DNA to left-handed Z-DNA, Eur J Biochem 206 (1992) 49-58.

[84] V. Svetlov, D.G. Vassylyev, I. Artsimovitch, Discrimination against deoxyribonucleotide substrates by bacterial RNA polymerase, J Biol Chem 279 (2004) 38087-38090.

[85] J. Acker, M. Wintzerith, M. Vigneron, C. Kedinger, Structure of the gene encoding the 14.5 kDa subunit of human RNA polymerase II, Nucleic Acids Res 21 (1993) 5345-5350.

[86] P.V. Shcherbakova, Y.I. Pavlov, O. Chilkova, I.B. Rogozin, E. Johansson, T.A. Kunkel, Unique error signature of the four-subunit yeast DNA polymerase epsilon, J Biol Chem 278 (2003) 43770-43780.

[87] E.M. Furter-Graves, B.D. Hall, R. Furter, Role of a small RNA pol II subunit in TATA to transcription start site spacing, Nucleic Acids Res 22 (1994) 4932-4936.

[88] M.H. Jenks, T.W. O'Rourke, D. Reines, Properties of an intergenic terminator and start site switch that regulate IMD2 transcription in yeast, Mol Cell Biol 28 (2008) 3883-3893.

[89] S.A. Nick McElhinny, B.E. Watts, D. Kumar, D.L. Watt, E.B. Lundstrom, P.M. Burgers, E. Johansson, A. Chabes, T.A. Kunkel, Abundant ribonucleotide incorporation into DNA by yeast replicative polymerases, Proc Natl Acad Sci U S A 107 (2010) 4949-4954.

[90] Y. Huang, R.V. Intine, A. Mozlin, S. Hasson, R.J. Maraia, Mutations in the RNA polymerase III subunit Rpc11p that decrease RNA 3' cleavage activity increase 3'-terminal oligo(U) length and La-dependent tRNA processing, Mol Cell Biol 25 (2005) 621-636.

[91] G. Cipres-Palacin, C.M. Kane, Cleavage of the nascent transcript induced by TFIIS is insufficient to promote read-through of intrinsic blocks to elongation by RNA polymerase II, Proc Natl Acad Sci U S A 91 (1994) 8087-8091.